AD

USAAVLABS TECHNICAL REPORT 71-10

THE EFFECTS OF INTERLAMINAR SHEAR ON THE BENDING AND BUCKLING OF FIBER-REINFORCED, COMPOSITE, FLAT AND CURVED PLATES

By

H. Durlofsky
J. Mayers

May 1971

EUSTIS DIRECTORATE
U. S. ARMY AIR MOBILITY RESEARCH AND DEVELOPMENT LABORATORY
FORT EUSTIS, VIRGINIA

CONTRACT DAAJ02-70-C-0075
DEPARTMENT OF AERONAUTICS AND ASTRONAUTICS
STANFORD UNIVERSITY
STANFORD, CALIFORNIA

DISCLAIMERS

The findings in this report are not to be construed as an official Department of the Army position unless so designated by other authorized documents.

When Government drawings, specifications, or other data are used for any purpose other than in connection with a definitely related Government procurement operation, the United States Government thereby incurs no responsibility nor any obligation whatsoever; and the fact that the Government may have formulated, furnished, or in any way supplied the said drawings, specifications, or other data is not to be regarded by implication or otherwise as in any manner licensing the holder or any other person or corporation, or conveying any rights or permission, to manufacture, use, or sell any patented invention that may in any way be related thereto.

DISPOSITION INSTRUCTIONS

Destroy this report when no longer needed. Do not return it to the originator.

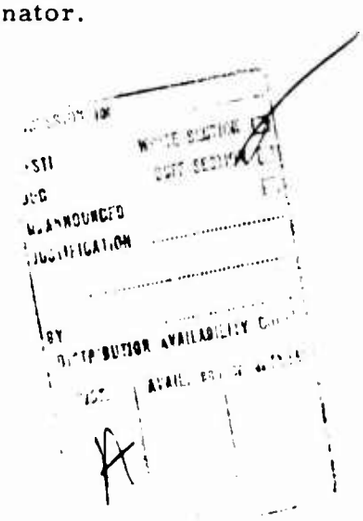

UNCLASSIFIED

Security Classification

DOCUMENT CONTROL DATA - R & D

(Security classification of title, body of abstract and indexing annotation must be entered when the overall report is classified)

1. ORIGINATING ACTIVITY *(Corporate author)* Stanford University Department of Aeronautics and Astronautics Stanford, California	2a. REPORT SECURITY CLASSIFICATION UNCLASSIFIED 2b. GROUP N/A

3. REPORT TITLE

THE EFFECTS OF INTERLAMINAR SHEAR ON THE BENDING AND BUCKLING OF FIBER-REINFORCED, COMPOSITE, FLAT AND CURVED PLATES

4. DESCRIPTIVE NOTES *(Type of report and inclusive dates)*
Final Report

5. AUTHOR(S) *(First name, middle initial, last name)*

Harold Durlofsky
Jean Mayers

6. REPORT DATE	7a. TOTAL NO. OF PAGES	7b. NO. OF REFS
May 1971	80	18

8a. CONTRACT OR GRANT NO. DAAJ02-70-C-0075	9a. ORIGINATOR'S REPORT NUMBER(S) USAAVIABS Technical Report 71-10
b. PROJECT NO. Task 1F061102A33F02	
c.	9b. OTHER REPORT NO(S) *(Any other numbers that may be assigned this report)*
d.	

10. DISTRIBUTION STATEMENT

Approved for public release; distribution unlimited.

11. SUPPLEMENTARY NOTES	12. SPONSORING MILITARY ACTIVITY
	Eustis Directorate, U.S. Army Air Mobility Research and Development Laboratory Fort Eustis, Virginia

13. ABSTRACT

A small deflection plate theory is developed which includes higher order approximations to the effects of transverse shear. The governing equations and associated boundary conditions are developed by a variational method. The theory is sufficiently general to encompass anisotropic, laminated, composite, circularly curved, cylindrical plate elements of nonsymmetric cross section. Specific applications are made to the bending and the axial compression buckling of simply supported flat plates and to the axial compression buckling of curved plates and shells having classical, simple supports. It is shown that the effects of interlaminar shear can be significant in composite constructions which use very high strength fiber reinforcement.

DD FORM 1 NOV 68 1473 REPLACES DD FORM 1473, 1 JAN 64, WHICH IS OBSOLETE FOR ARMY USE.

UNCLASSIFIED

Security Classification

14. KEY WORDS	LINK A		LINK B		LINK C	
	ROLE	WT	ROLE	WT	ROLE	WT
Plate Structures						
Shell Structures						
Bending						
Stability						
Fiber-Reinforced Composite Structures						
Anisotropic Structures						

DEPARTMENT OF THE ARMY
U. S. ARMY AIR MOBILITY RESEARCH & DEVELOPMENT LABORATORY
EUSTIS DIRECTORATE
FORT EUSTIS, VIRGINIA 23604

This program was conducted under Contract DAAJ02-70-C-0075 with Stanford University, Stanford, California.

The data contained in this report are the result of research efforts to develop the theory for analyzing the effects of interlaminar shear on the bending and buckling of fiber-reinforced, composite, flat and curved plates. The theory is sufficiently general to encompass anisotropic, laminated elements of nonsymmetric cross section.

The report has been reviewed by this Directorate and is considered to be technically sound. It is published for the exchange of information and the stimulation of future research.

This program was conducted under the technical management of Mr. James P. Waller, Structures Division.

Task 1F061102A33F02
Contract DAAJ02-70-C-0075
USAAVLABS Technical Report 71-10
May 1971

THE EFFECTS OF INTERLAMINAR SHEAR ON THE BENDING AND BUCKLING OF FIBER-REINFORCED, COMPOSITE, FLAT AND CURVED PLATES

Final Report

By

H. Durlofsky
J. Mayers

Prepared by

Department of Aeronautics and Astronautics
Stanford University
Stanford, California

for

EUSTIS DIRECTORATE
U.S. ARMY AIR MOBILITY RESEARCH AND DEVELOPMENT LABORATORY
FORT EUSTIS, VIRGINIA

SUMMARY

A small deflection plate theory is developed which includes higher order approximations to the effects of transverse shear. The governing equations and associated boundary conditions are developed by a variational method. The theory is sufficiently general to encompass anisotropic, laminated, composite, circularly curved, cylindrical plate elements of nonsymmetric cross section. Specific applications are made to the bending and the axial compression buckling of simply supported flat plates and to the axial compression buckling of curved plates and shells having classical, simple supports. It is shown that the effects of interlaminar shear can be significant in composite constructions which use very high strength fiber reinforcement.

FOREWORD

The work reported herein constitutes a portion of a continuing effort being undertaken at Stanford University for the Eustis Directorate, U.S. Army Air Mobility Research and Development Laboratory under Contract DAAJ02-70-C-0075 (Project 1F061102A33F) to establish accurate theoretical prediction capability for the static and dynamic behavior of aircraft structural components using both conventional and unconventional materials. Predecessor contracts supported investigations which led, in part, to the results presented in References 10, 11, 14, and 15.

BLANK PAGE

TABLE OF CONTENTS

TABLE OF CONTENTS (Cont'd)

LIST OF ILLUSTRATIONS

LIST OF SYMBOLS

A_{ij}, B_{ij}, D_{ij}	plate constants defined by Equations (89)
$\tilde{A}$	$n \times n$ matrix defined by Equation (13)
$\tilde{A}^*$	$(n + 1) \times (n + 1)$ matrix defined by Equation (26)
$\vec{B}$	n-dimensional vector defined by Equation (12)
$\vec{B}^*$	$(m + 1)$-dimensional vector defined by Equation (27)
b	dimension of plate at median surface in y-direction, in.
C_{ij}	material constant, lb/in.^{2}
$C_{ij}^{(k)}$	element of k^{th} lamina constitutive law matrix, lb/in.^{2}
$\tilde{C}_{ij}$	$n \times n$ matrix of material elastic constants defined by Equation (14)
$\tilde{C}_{ij}^*$	$(m + 1) \times (m + 1)$ transformed matrix of material elastic constants defined by Equation (25)
D	bending stiffness of homogeneous plate, lb-in.
E	Young's modulus of homogeneous plate, lb/in.^{2}
E_{11}, E_{22}	extensional moduli of composite material, lb/in.^{2}
e_{ij}, f_{ij}, g_j	arbitrary displacement coefficients, in.
$\vec{e}, \vec{f}, \vec{g}$	vectors of arbitrary displacement coefficients, in.
G_{12}	inplane laminae shear modulus, lb/in.^{2}
G_B	interlaminar shear modulus, lb/in.^{2}
h	dimension of plate in z-direction, in.
$\vec{I}$	n-dimensional unit vector

$\vec{K}_{ij}$	(m + 1)-dimensional vector defined by Equation (28)
L	dimension of plate at median surface in x-direction, in.
m	degree of approximation of distribution of inplane displacement functions through plate thickness
N_x	axial compression loading, lb/in.
n	number of laminae
p	surface loading, lb/in.^{2}
p_0	intensity of surface loading, lb/in.^{2}
$\tilde{Q}$	n × (n + 1) transformation matrix defined by Equation (24)
R	radius of curvature, in.
$\tilde{S}_j$	matrix of integrated minimizing functions defined by Equations (83)
t	lamina thickness, in.
U	total strain energy, lb-in.
U_s	strain energy due to interlaminar shear, lb-in.
u_k, v_k	median surface displacement functions of k^{th} lamina, in.
$\vec{u}, \vec{v}$	n-dimensional displacement vectors
u^*, v^*	generalized displacement functions
$\vec{u}^*, \vec{v}^*$	(m + 1)-dimensional generalized displacement vectors
V	potential of applied loads, lb-in.
w	lateral displacement function of laminate, in.
x,y,z	plate coordinates, in.
α, β, γ	minimizing functions

α,β,γ	vectors of minimizing functions
$\tilde{\alpha},\tilde{\beta}$	matrices of minimizing functions
$\gamma_{xy}^{(k)}$	median surface shearing strains of k^{th} laminae, in./in.
$\gamma_{xz}^{(k)},\gamma_{yz}^{(k)}$	interlaminar shearing strains acting between the median surfaces of the k and $k+1$ laminae, in./in.
Δ	maximum plate deflection, in.
Δ_0	maximum plate deflection for plate with $G_B/E_{11} \rightarrow 1$, in.
δ	variational operator
$\epsilon_x^{(k)},\epsilon_y^{(k)}$	median surface extensional strains of k^{th} laminae, in./in.
θ	angle between lamina natural axes and coordinate axes, deg
ν	Poisson's ratio for homogeneous plate
ν_{12}	Poisson's ratio for anisotropic laminae
$\tilde{\Phi}_j$	matrix of product of minimizing functions defined by Equations (80)
$\sigma_x^{(k)},\sigma_y^{(k)}$	median surface extensional stress of k^{th} lamina, lb/in.^{2}
σ_{cr}	critical axial compressive stress, lb/in.^{2}
$(\sigma_{cr})_0$	critical axial compressive stress for plate having $G_B/E_{11} \rightarrow 1$, lb/in.^{2}
$\tau_{xy}^{(k)}$	median surface shearing stress of k^{th} lamina, lb/in.^{2}
$\tau_{xz}^{(k)},\tau_{yz}^{(k)}$	interlaminar shearing stress acting between the median surfaces of the k and $k+1$ laminae, lb/in.^{2}
ψ	change in fiber orientation between adjacent laminae, deg

SUPERSCRIPTS

(k)	k^{th} lamina
T	transpose
$*$	transformed quantity
$\sim$	matrix
$\rightarrow$	vector

BLANK PAGE

INTRODUCTION

The desire for significantly increased efficiency in aerospace structures has encouraged the development of high-strength fiber composites for use in laminated plate and shell elements. However, to realize the potential inherent in composite construction, the theoretical prediction capability must be improved in order to match laboratory experience. Plate and shell theories which deal selectively with only some of the characteristics of laminated, composite constructions are becoming inadequate for the very high strength fiber composites being developed. In the case of laminated plates and shells, researchers[1-4] have been concerned primarily with the anisotropic nature of layered constructions under the assumption that the interlaminar shear effects are negligible. Whereas this assumption is reasonably valid for composites with relatively high ratios of interlaminar shear to laminae extensional moduli (for example, glass-epoxy), there is reason to question this assumption for some of the newer composites (for example, boron-epoxy) wherein relatively low ratios of these moduli exist.

The literature on the bending and buckling of laminated, composite plates and shells may be considered to begin with the work of Smith (Reference 1). Therein, Smith considered the bending of a two-layered rectangular plate with orthotropic layers oriented so that the natural axes of each layer made equal but opposite angles with the coordinate axes. Plates and shells of this construction are referred to as being of the Smith type. By overlooking coupling between bending and membrane stresses, Smith concluded erroneously that a plate of this construction behaves in the same manner as the conventional orthotropic plate. Reissner and Stavsky[2] formulated the composite plate problem in terms of an Airy stress function and the lateral deflection. For the Smith-type plate, they established the existence of interaction between bending and extensional stresses in plates under direct and lateral loads, respectively. In laminated plates symmetrical about a median surface, this coupling vanishes. In addition, Reissner and Stavsky noted from their solution that when the angle between the coordinate and laminae natural axes is 45 degrees in a Smith-type plate, the membrane shear rigidity has no effect on the solution.

In Reference 3, the authors extended the Reissner-Stavsky formulation to shells; they applied their solution to a circular, cylindrical, composite shell of Smith-type construction subjected to internal pressure. The coupling phenomenon found in the plate analysis[2] was present also in that of the shell. The authors considered the validity of the Donnell approximations[5] when applied to composite shells and concluded that except for highly anisotropic composites ($E_{11}/E_{22} > 1000$), any error introduced into composite-shell theory above that introduced into classical shell theory is negligible. Whitney and Leissa[4] reformulated the anisotropic plate problem in terms of the inplane and lateral displacements, and the stress resultants. They examined several bending, stability, and vibration problems not previously considered.

The principal thrust of the foregoing studies was to show the effects of laminae anisotropy and variations in laminae orientations on the behavior of composite plates and shells. As all of the solutions relied on the Kirchhoff-Love hypothesis, the effects of interlaminar shear were neglected entirely. With regard to interlaminar shear effects, Pagano[6] pointed out their importance in discussing the differences between the flexural and extensional moduli of composite materials. He used an approximate method of Hoff (see Reference 6) in calculating the effect of shear on lateral deflections for the special case of bidirectional composite beams in cylindrical bending.

A more rigorous analysis of interlaminar shear effects in the bending of composite plates was presented by Whitney.[7] This solution was based on the anisotropic plate equations, including the effects of transverse shear, developed by Ambartsumyan.[8] Whitney modified the Ambartsumyan equations to accommodate composite plates, and he also included coupling between the two transverse shearing strains not present in the Ambartsumyan formulation. The solutions obtained by Whitney were applicable primarily to composite plates symmetrical about a median plane; for unsymmetrical constructions he considered only a plate strip. In addition, Whitney's results were confined to the consideration of the effects of large length-to-thickness ratios.

By extending the work of Khot[9] to include a first approximation to the effects of interlaminar shear, Taylor and Mayers[10] obtained solutions for axial compression buckling of composite, circular, cylindrical shells. In their analysis, Taylor and Mayers used a modified-Reissner variational principle[11] in conjunction with the constitutive and strain-displacement relations given in Reference 3 and the curvature relations analogous to those used in Reference 12. Results were obtained for boron- and glass-epoxy cylinders.

The theoretical development and analysis presented herein take an essentially different approach from all of the foregoing. These formulations were based on classical plate theory in that they used the equations of motion in terms of stress resultants and the Kirchhoff-Love hypothesis to establish the governing equations. By contrast, the present analysis, suggested by the sandwich-plate developments given in References 13 and 14, makes use of nonclassical kinematics and a variational principle to establish the governing equations and associated boundary conditions. The total potential energy developed in a composite plate during bending is formulated in terms of the displacements, and the variation with respect to the independent displacement functions yields the governing differential equations and boundary conditions in accordance with the potential energy principle.

The model used is a generalization of that of Hoff in Reference 13 for sandwich plates. Hoff's model consisted of a core enclosed by two membrane face sheets. The core was considered to extend to the median planes of the two face sheets and to carry only transverse shear. The behavior of two adjacent laminae in a composite plate can be represented by a similar model under the following assumptions:

1. The laminae behave as anisotropic membranes with all of the direct stress carrying material located at the median surfaces.
2. The matrix material between adjacent median surfaces carries all of the transverse shear.

Hence, the composite plate is considered to be a multilayered sandwich plate with the matrix material acting as cores and the matrix-fiber combination acting as the membranes. It should be noted that the matrix

is considered to carry two types of stresses which do not couple: the matrix acts in conjunction with the fibers to transmit the laminae stresses, and it acts alone to resist the stresses due to transverse shear.

For ease of analysis, compared with the methods, for example, of References 2, 3, and 4, a vector-matrix technique is introduced. The inplane displacements of the laminated plate are described by two sets of functions, u_k and v_k $(k = 1,2,\ldots,n)$, where k designates any one of the n layers. These sets of functions are considered to constitute two n-dimensional vectors over the vector field of the plate reference surface, and the total potential energy is formulated in terms of these two vectors and the lateral displacement function, w. Approximations to any degree of accuracy of the two vectors are then introduced by means of linear transformations. These approximations give the two sets of displacement functions in terms of smaller sets of generalized displacement functions. The Euler equations and all associated boundary conditions are then developed in terms of the approximated vectors and the lateral displacement. Actually, the Euler equations corresponding to the two vector quantities are, in effect, sets of scalar equations involving the generalized displacement functions describing the plate behavior. The theory is not restricted to the preservation of plane sections and can be extended readily to include the definition of a separate lateral deflection function for each lamina. This approach was adopted in Reference 15 in studying the bending and buckling of layered beams. Results of the analysis for several bending and buckling problems of plate and shell elements are presented in the form of charts. Details of all theoretical developments appear in the appendixes.

BASIC THEORY

STATEMENT OF PROBLEM AND BASIC ASSUMPTIONS

The problem considered is the effect of interlaminar shear on the bending and buckling of composite, flat plates and circularly curved cylindrical shells.

The composite structures are considered to consist of n laminae of equal thickness, with each lamina composed of a matrix of finite shear transmissibility reinforced by continuous fibers in two perpendicular directions. The fiber orientation may be different for different layers.

The analytical model (see Figure 1) consists of n homogeneous, anisotropic laminae. Two tangent-plane displacement functions, u_k and v_k ($k = 1,2,\ldots,n$) are assigned to each lamina. In addition, there is a lateral displacement function, w, common to all n laminae. The radius of curvature, R, is considered to be the same for all laminae and equal to the radius of the laminate median surface.

Each lamina is assumed to be in a state of plane stress. In the transverse planes, only shearing stresses are considered; all other stresses are assumed to be negligible. The transverse shearing stresses are assumed to be carried by the matrix material. No restriction is placed on the preservation of plane sections. Finally, the lateral deflections of the composite structure are assumed to be small in comparison with its overall thickness.

STRAIN-DISPLACEMENT RELATIONS FOR A LAMINA

For each lamina, when the Donnell[5] approximations are used, the strain-displacement relations can be expressed as

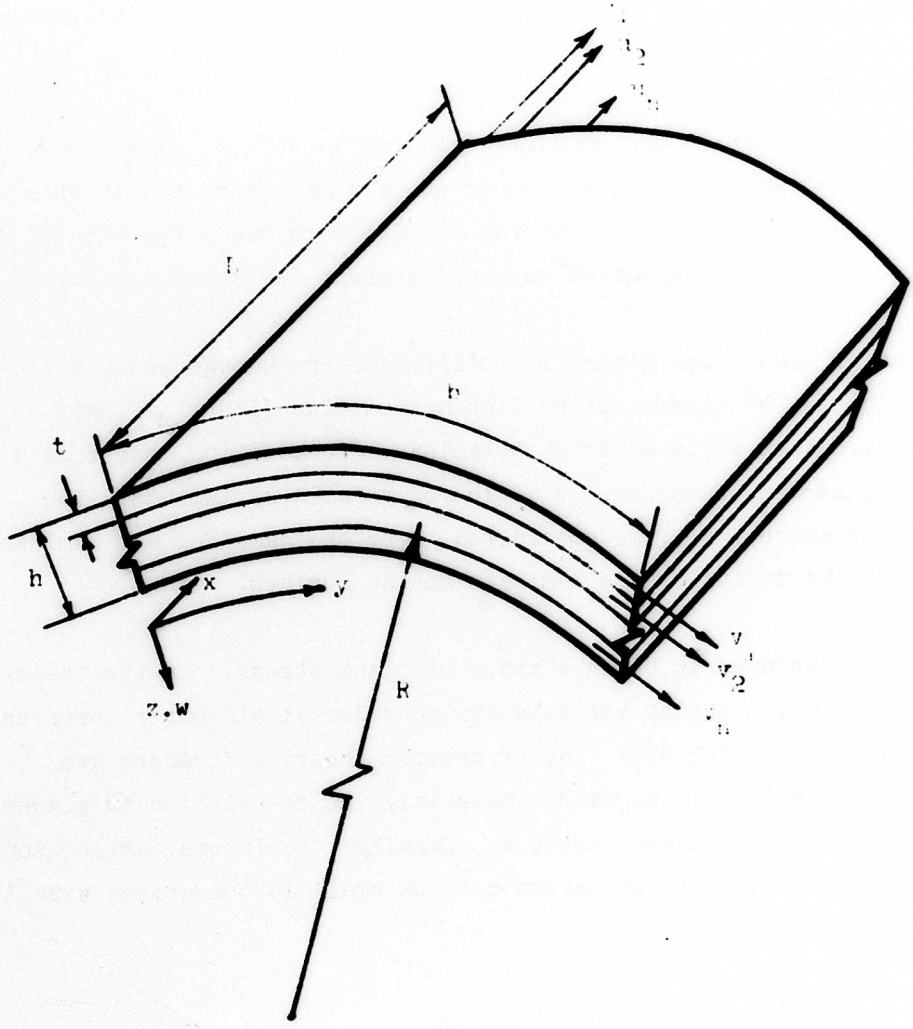

Figure 1. Analytical Model of Composite Plate.

$$\left.\begin{aligned} \epsilon_x^{(k)} &= \frac{\partial u_k}{\partial x}, \quad \epsilon_y^{(k)} = \frac{\partial v_k}{\partial y} - \frac{w}{R} \\ \gamma_{xy}^{(k)} &= \frac{\partial u_k}{\partial y} + \frac{\partial v_k}{\partial x} \end{aligned}\right\} \tag{1}$$

where, as shown in Figure 1, the radial displacement is positive when directed **inwardly.**

TRANSVERSE SHEAR STRAIN-DISPLACEMENT RELATIONS BETWEEN ADJACENT LAMINAE

As derived in Appendix I, the transverse shear strains between adjacent laminae are given in terms of the inplane and lateral displacement functions of the k and $k+1$ laminae as

$$\left.\begin{aligned} \gamma_{xz}^{(k)} &= \frac{\partial w}{\partial x} - \frac{u_k - u_{k+1}}{t} \\ \gamma_{yz}^{(k)} &= \frac{\partial w}{\partial y} - \frac{v_k - v_{k+1}}{t} \end{aligned}\right\} \tag{2}$$

CONSTITUTIVE RELATIONS FOR A LAMINA

The relations between the inplane stresses and strains are those which govern the behavior of a homogeneous, anisotropic medium in a state of plane stress. In matrix notation, these relations are[16]

$$\begin{bmatrix} \sigma_x^{(k)} \\ \sigma_y^{(k)} \\ \tau_{xy}^{(k)} \end{bmatrix} = \begin{bmatrix} C_{11}^{(k)} & C_{12}^{(k)} & C_{13}^{(k)} \\ C_{12}^{(k)} & C_{22}^{(k)} & C_{23}^{(k)} \\ C_{13}^{(k)} & C_{23}^{(k)} & C_{33}^{(k)} \end{bmatrix} \cdot \begin{bmatrix} \epsilon_x^{(k)} \\ \epsilon_y^{(k)} \\ \gamma_{xy}^{(k)} \end{bmatrix} \tag{3}$$

where the matrix elements, $C_{ij}^{(k)}$, are related to the engineering material constants by[16]

$$\left.\begin{aligned}
C_{11}^{(k)} &= C_{11}\cos^4\theta + 2(C_{12} + 2C_{33})\sin^2\theta\cos^2\theta + C_{22}\sin^4\theta \\
C_{12}^{(k)} &= (C_{11} + C_{22} - 4C_{33})\sin^2\theta\cos^2\theta + C_{12}(\sin^4\theta + \cos^4\theta) \\
C_{13}^{(k)} &= (C_{11} - C_{12} - 2C_{33})\sin\theta\cos^3\theta \\
&\quad + (C_{12} - C_{22} + 2C_{33})\sin^3\theta\cos\theta \\
C_{22}^{(k)} &= C_{11}\sin^4\theta + 2(C_{12} + 2C_{33})\sin^2\theta\cos^2\theta + C_{22}\cos^4\theta \\
C_{23}^{(k)} &= (C_{11} - C_{12} - 2C_{33})\sin^3\theta\cos\theta \\
&\quad + (C_{12} - C_{22} + 2C_{33})\sin\theta\cos^3\theta \\
C_{33}^{(k)} &= (C_{11} + C_{22} - 2C_{12} - 2C_{33})\sin^2\theta\cos^2\theta \\
&\quad + C_{33}(\sin^4\theta + \cos^4\theta)
\end{aligned}\right\} \quad (4)$$

and

$$\left.\begin{aligned}
C_{11} &= \frac{E_{11}}{1 - \nu_{12}^2} \\
C_{12} &= \frac{E_{11}\,\nu_{12}}{1 - \nu_{12}^2} \\
C_{22} &= \frac{E_{22}}{1 - \nu_{12}^2} \\
C_{33} &= G_{12}
\end{aligned}\right\} \quad (5)$$

POTENTIAL ENERGY FORMULATION

Strain Energy

The strain energy stored in a laminated, circularly curved plate consists of the strain energy associated with the plane state of stress of the laminae as developed in the classical manner from Equations (1) and (3), and the strain energy due to transverse shear as derived in Appendix I.

Thus, the strain energy is expressed in terms of the displacements as

$$U = \sum_{k=1}^{n} \frac{t}{2} \int_0^L \int_0^b \left\{ \left[C_{11}^{(k)} \frac{\partial u_k}{\partial x} + C_{12}^{(k)} \left(\frac{\partial v_k}{\partial y} - \frac{w}{R} \right) + C_{13}^{(k)} \left(\frac{\partial u_k}{\partial y} + \frac{\partial v_k}{\partial x} \right) \right] \frac{\partial u_k}{\partial x} \right.$$

$$+ \left[C_{12}^{(k)} \frac{\partial u_k}{\partial x} + C_{22}^{(k)} \left(\frac{\partial v_k}{\partial y} - \frac{w}{R} \right) + C_{23}^{(k)} \left(\frac{\partial u_k}{\partial y} + \frac{\partial v_k}{\partial x} \right) \right] \left(\frac{\partial v_k}{\partial y} - \frac{w}{R} \right)$$

$$\left. + \left[C_{13}^{(k)} \frac{\partial u_k}{\partial x} + C_{23}^{(k)} \left(\frac{\partial v_k}{\partial y} - \frac{w}{R} \right) + C_{33}^{(k)} \left(\frac{\partial u_k}{\partial y} + \frac{\partial v_k}{\partial x} \right) \right] \left(\frac{\partial u_k}{\partial y} + \frac{\partial v_k}{\partial x} \right) \right\} dxdy$$

$$+ \sum_{k=1}^{n-1} \frac{G_B t}{2} \int_0^L \int_0^b \left[\left(\frac{\partial w}{\partial x} - \frac{u_k - u_{k+1}}{t} \right)^2 + \left(\frac{\partial w}{\partial y} - \frac{v_k - v_{k+1}}{t} \right)^2 \right] dxdy \qquad (6)$$

Potential of Applied Loads

Two types of loadings are considered as shown in Figure 2: distributed, lateral surface loadings, and compressive edge loadings along the edges $x = 0$ and $x = b$. The potential of the applied loads for the two cases is given, respectively, by

$$\left. \begin{aligned} V &= -\int_0^L \int_0^b [pw] \, dxdy \\ \text{and} \\ V &= -\int_0^L \int_0^b \left[\frac{N_x}{2} \left(\frac{\partial w}{\partial x} \right)^2 \right] dxdy \end{aligned} \right\} \qquad (7)$$

In the first of Equations (7), w is the total displacement measured from the undeformed state, whereas in the second of Equations (7), w is the additional displacement which occurs during a buckling process.

Total Potential Energy

The total potential energy is given by Equations (6) and (7), with either $N_x = 0$ for bending problems or $p = 0$ for axial compression buckling

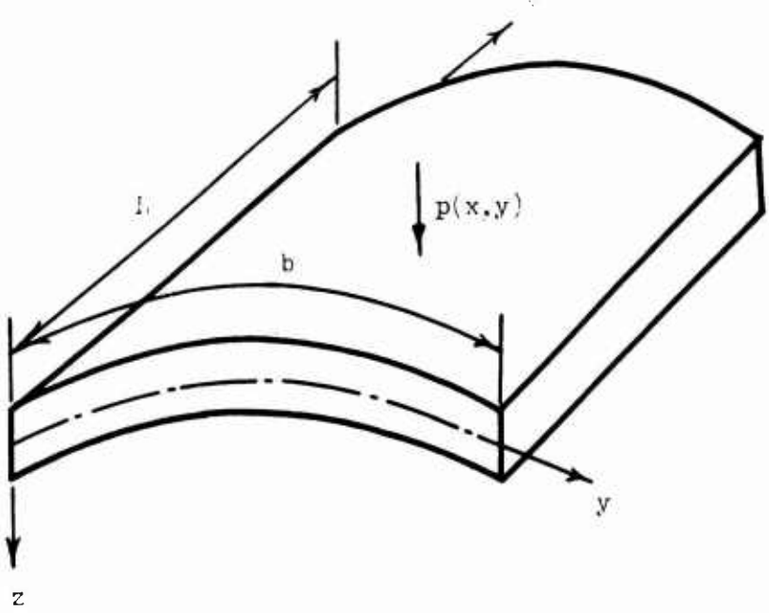

Distributed Lateral Loading

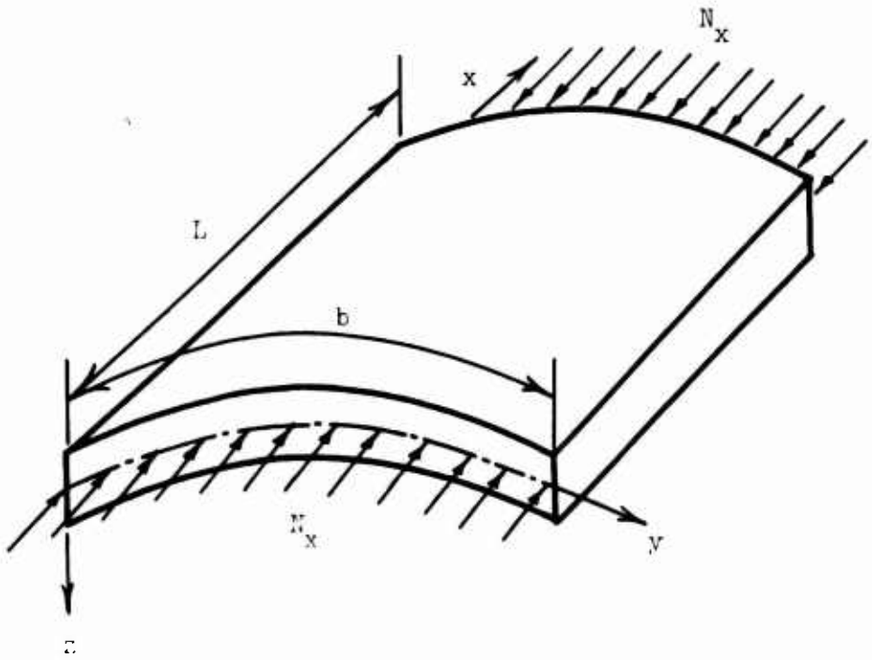

Uniform Axial Compression Loading

Figure 2. Plate Loading Cases.

problems, as

$$U + V = \sum_{k=1}^{n} \frac{t}{2} \int_0^L \int_0^b \left\{ \left[C_{11}^{(k)} \frac{\partial u_k}{\partial x} + C_{12}^{(k)} \left(\frac{\partial v_k}{\partial y} - \frac{w}{R} \right) + C_{13}^{(k)} \left(\frac{\partial u_k}{\partial y} + \frac{\partial v_k}{\partial x} \right) \right] \frac{\partial u_k}{\partial x} \right.$$

$$+ \left[C_{12}^{(k)} \frac{\partial u_k}{\partial x} + C_{22}^{(k)} \left(\frac{\partial v_k}{\partial y} - \frac{w}{R} \right) + C_{23}^{(k)} \left(\frac{\partial u_k}{\partial y} + \frac{\partial v_k}{\partial x} \right) \right] \cdot \left(\frac{\partial v_k}{\partial y} - \frac{w}{R} \right)$$

$$\left. + \left[C_{13}^{(k)} \frac{\partial u_k}{\partial x} + C_{23}^{(k)} \left(\frac{\partial v_k}{\partial y} - \frac{w}{R} \right) + C_{33}^{(k)} \left(\frac{\partial u_k}{\partial y} + \frac{\partial v_k}{\partial x} \right) \right] \cdot \left(\frac{\partial u_k}{\partial y} + \frac{\partial v_k}{\partial x} \right) \right\} dxdy$$

$$+ \sum_{k=1}^{n-1} \frac{G_B t}{2} \int_0^L \int_0^b \left[\left(\frac{\partial w}{\partial x} - \frac{u_k - u_{k+1}}{t} \right)^2 + \left(\frac{\partial w}{\partial y} - \frac{v_k - v_{k+1}}{t} \right)^2 \right] dxdy$$

$$- \int_0^L \int_0^b [pw] \, dxdy - \int_0^L \int_0^b \left[\frac{N_x}{2} \left(\frac{\partial w}{\partial x} \right)^2 \right] dxdy \qquad (8)$$

TOTAL POTENTIAL ENERGY IN VECTOR-MATRIX NOTATION

The total potential energy as given by Equation (8) involves $2n + 1$ displacement functions, u_k and v_k $(k = 1,2,\ldots,n)$, and the lateral displacement function w. From Equation (8), it can be seen that the set of displacement functions u_k is subjected to the same differential and integral operations. This consideration also applies to the set of displacement functions v_k. Consequently, it is advantageous to consider these sets of functions as constituting two n-dimensional vectors, $\vec{u}$ and $\vec{v}$, and to formulate the total potential energy as given by Equation (8) in vector-matrix notation. This allows the subsequent operations of variation and integration to be carried out with respect to the two displacement vectors $\vec{u}$ and $\vec{v}$ rather than the $2n$ displacement functions u_k and v_k. With

$$\vec{u} = \begin{bmatrix} u_1 \\ u_2 \\ \cdot \\ \cdot \\ \cdot \\ u_n \end{bmatrix} \qquad (9)$$

$$\vec{v} = \begin{bmatrix} v_1 \\ v_2 \\ \cdot \\ \cdot \\ \cdot \\ v_n \end{bmatrix} \tag{10}$$

$$\vec{I} = \begin{bmatrix} 1 \\ 1 \\ \cdot \\ \cdot \\ \cdot \\ 1 \end{bmatrix} \tag{11}$$

$$\vec{B} = \begin{bmatrix} 1 \\ 0 \\ \cdot \\ \cdot \\ \cdot \\ 0 \\ -1 \end{bmatrix} \tag{12}$$

$$\tilde{A} = \begin{bmatrix} 1 & -1 & 0 & 0 & \cdots & 0 \\ -1 & 2 & -1 & 0 & \cdots & 0 \\ 0 & -1 & 2 & -1 & 0 & \cdots \\ \cdot & & & & & \\ \cdot & & & & & \\ \cdot & & & & & \\ 0 & \cdots & 0 & -1 & 2 & -1 \\ 0 & \cdots & 0 & 0 & -1 & 1 \end{bmatrix} \tag{13}$$

and

$$\tilde{C}_{ij} = \begin{bmatrix} C_{ij}^{(1)} & 0 & 0 & \cdots & 0 \\ 0 & C_{ij}^{(2)} & 0 & \cdots & 0 \\ \vdots & & & & \\ 0 & 0 & \cdots & 0 & C_{ij}^{(n)} \end{bmatrix}_{\substack{i=1,2,3 \\ j=1,2,3}} \tag{14}$$

the total potential energy can be written now as

$$\begin{aligned} U + V = \frac{t}{2} \int_0^L \int_0^b \Bigg\{ & \left[\tilde{C}_{11} \cdot \frac{\partial \vec{u}}{\partial x} + \tilde{C}_{12} \cdot \left(\frac{\partial \vec{v}}{\partial y} - \frac{w}{R} \vec{I} \right) \right. \\ & + \left. \tilde{C}_{13} \cdot \left(\frac{\partial \vec{u}}{\partial y} + \frac{\partial \vec{v}}{\partial x} \right) \right]^T \cdot \frac{\partial \vec{u}}{\partial x} + \left[\tilde{C}_{12} \cdot \frac{\partial \vec{u}}{\partial x} + \tilde{C}_{22} \cdot \left(\frac{\partial \vec{v}}{\partial y} - \frac{w}{R} \vec{I} \right) \right. \\ & + \left. \tilde{C}_{23} \cdot \left(\frac{\partial \vec{u}}{\partial y} + \frac{\partial \vec{v}}{\partial x} \right) \right]^T \cdot \left(\frac{\partial \vec{v}}{\partial y} - \frac{w}{R} \vec{I} \right) + \left[\tilde{C}_{13} \cdot \frac{\partial \vec{u}}{\partial x} \right. \\ & + \left. \tilde{C}_{23} \cdot \left(\frac{\partial \vec{v}}{\partial y} - \frac{w}{R} \vec{I} \right) + \tilde{C}_{33} \cdot \left(\frac{\partial \vec{u}}{\partial y} + \frac{\partial \vec{v}}{\partial x} \right) \right]^T \cdot \left(\frac{\partial \vec{u}}{\partial y} + \frac{\partial \vec{v}}{\partial x} \right) \Bigg\} \, dxdy \\ & + \frac{G_B t}{2} \int_0^L \int_0^b \Bigg\{ (n-1) \left[\left(\frac{\partial w}{\partial x} \right)^2 + \left(\frac{\partial w}{\partial y} \right)^2 \right] - \frac{2}{t} \frac{\partial w}{\partial x} \vec{B}^T \cdot \vec{u} \\ & + \frac{1}{t^2} \vec{u}^T \cdot \tilde{A} \cdot \vec{u} - \frac{2}{t} \frac{\partial w}{\partial y} \vec{B}^T \cdot \vec{v} + \frac{1}{t^2} \vec{v}^T \cdot \tilde{A} \cdot \vec{v} \Bigg\} \, dxdy \\ & - \int_0^L \int_0^b [pw] \, dxdy - \int_0^L \int_0^b \left[\frac{N_x}{2} \left(\frac{\partial w}{\partial x} \right)^2 \right] dxdy \end{aligned} \tag{15}$$

REDUCTION OF INDEPENDENT DISPLACEMENT FUNCTIONS IN TOTAL POTENTIAL ENERGY

As shown in detail in Appendix II, the set of displacement functions u_k $(k = 1,2,\ldots,n)$ may be considered as related by

$$u_k(x,y) = F_1(x,y,z_k) \qquad k = 1,2,\ldots,n \tag{16}$$

where z_k is the distance from any arbitrary reference plane to the center of the k^{th} lamina. When the function F_1 is approximated by the first $m + 1$ terms of its power series expansion in z as

$$F_1(x,y,z) = u_0^*(x,y) + zu_1^*(x,y) + \ldots + z^m u_m^*(x,y) \tag{17}$$

the displacement functions u_k given by Equation (16) become

$$u_k = u_0^* + z_k u_1^* + \ldots + z_k^m u_m^* \qquad k = 1,2,\ldots,n \tag{18}$$

Similarly, the set of functions v_k can be approximated by

$$v_k = v_0^* + z_k v_1^* + \ldots + z_k^m v_m^* \qquad k = 1,2,\ldots,n \tag{19}$$

Equations (18) and (19) can effect a significant reduction in the number of independent displacement functions for multilayered plates with $n \gg 1$; these two sets of equations can be expressed in vector-matrix notation as, respectively,

$$\vec{u} = \tilde{Q} \cdot \vec{u}^* \tag{20}$$

and

$$\vec{v} = \tilde{Q} \cdot \vec{v}^* \tag{21}$$

where

$$\vec{u}^{\,*} = \begin{bmatrix} u_0^* \\ u_1^* \\ \vdots \\ u_m^* \end{bmatrix} \tag{22}$$

$$\vec{v}^{\,*} = \begin{bmatrix} v_0^* \\ v_1^* \\ \vdots \\ v_m^* \end{bmatrix} \tag{23}$$

$$\tilde{Q} = \begin{bmatrix} 1 & z_1 & z_1^2 & \cdots & z_1^m \\ 1 & z_2 & z_2^2 & \cdots & z_2^m \\ \vdots & & & & \\ 1 & z_n & z_n^2 & \cdots & z_n^m \end{bmatrix} \tag{24}$$

With

$$\tilde{C}_{ij}^{*} = \tilde{Q}^{T} \cdot \tilde{C}_{ij} \cdot \tilde{Q} \qquad \begin{matrix} i = 1,2,3 \\ j = 1,2,3 \end{matrix} \tag{25}$$

$$\tilde{A}^{*} = \tilde{Q}^{T} \cdot \tilde{A} \cdot \tilde{Q} \tag{26}$$

$$\vec{B}^{*} = \tilde{Q}^{T} \cdot \vec{B} \tag{27}$$

and

$$\vec{K}_{ij} = \tilde{Q}^{T} \cdot \tilde{C}_{ij} \cdot \vec{I} \qquad \begin{matrix} i = 1,2,3 \\ j = 1,2,3 \end{matrix} \tag{28}$$

the total potential energy as given by Equation (15) can be written in terms of $\vec{u}^{*}$ and $\vec{v}^{*}$ as

$$\begin{aligned} U + V = \frac{t}{2} \int_0^L \int_0^b \Bigg\{ & \left(\tilde{C}_{11}^{*} \cdot \frac{\partial \vec{u}^{*}}{\partial x} \right)^{T} \cdot \frac{\partial \vec{u}^{*}}{\partial x} + \left(\tilde{C}_{22}^{*} \cdot \frac{\partial \vec{v}^{*}}{\partial y} \right)^{T} \cdot \frac{\partial \vec{v}^{*}}{\partial y} \\ & + \left[\tilde{C}_{33}^{*} \cdot \left(\frac{\partial \vec{u}^{*}}{\partial y} + \frac{\partial \vec{v}^{*}}{\partial x} \right) \right]^{T} \cdot \left(\frac{\partial \vec{u}^{*}}{\partial y} + \frac{\partial \vec{v}^{*}}{\partial x} \right) + 2 \left(\tilde{C}_{12}^{*} \cdot \frac{\partial \vec{u}^{*}}{\partial x} \right)^{T} \cdot \frac{\partial \vec{v}^{*}}{\partial y} \\ & + 2 \left(\tilde{C}_{13}^{*} \cdot \frac{\partial \vec{u}^{*}}{\partial x} \right)^{T} \cdot \left(\frac{\partial \vec{u}^{*}}{\partial y} + \frac{\partial \vec{v}^{*}}{\partial x} \right) + 2 \left(\tilde{C}_{23}^{*} \cdot \frac{\partial \vec{v}^{*}}{\partial y} \right)^{T} \cdot \left(\frac{\partial \vec{u}^{*}}{\partial y} + \frac{\partial \vec{v}^{*}}{\partial x} \right) \\ & - \frac{2w}{R} \left[\vec{K}_{12}^{T} \cdot \frac{\partial \vec{u}^{*}}{\partial x} + \vec{K}_{23}^{T} \cdot \left(\frac{\partial \vec{v}^{*}}{\partial x} + \frac{\partial \vec{u}^{*}}{\partial y} \right) + \vec{K}_{22}^{T} \cdot \frac{\partial \vec{v}^{*}}{\partial y} \right] \\ & + \frac{w^2}{R^2} \left(\tilde{C}_{22}^{*} \cdot \vec{I} \right)^{T} \cdot \vec{I} \Bigg\} dxdy + \frac{G_B t}{2} \int_0^L \int_0^b \Bigg\{ (n-1) \left[\left(\frac{\partial w}{\partial x} \right)^2 + \left(\frac{\partial w}{\partial y} \right)^2 \right] \\ & - \frac{2}{t} \frac{\partial w}{\partial x} \vec{B}^{*T} \cdot \vec{u}^{*} + \frac{1}{t^2} \vec{u}^{*T} \cdot \tilde{A}^{*} \cdot \vec{u}^{*} - \frac{2}{t} \frac{\partial w}{\partial y} \vec{B}^{*T} \cdot \vec{v}^{*} \\ & + \frac{1}{t^2} \vec{v}^{*T} \cdot \tilde{A}^{*} \cdot \vec{v}^{*} \Bigg\} dxdy - \int_0^L \int_0^b [pw] \, dxdy - \int_0^L \int_0^b \left[\frac{N_x}{2} \left(\frac{\partial w}{\partial x} \right)^2 \right] dxdy \end{aligned} \tag{29}$$

where cognizance has been taken of the identities

$$\left.\begin{aligned} \tilde{\tilde{A}}^{*T} &\equiv \tilde{\tilde{A}}^{*} \\ \tilde{\tilde{C}}_{ij}^{*T} &\equiv \tilde{\tilde{C}}_{ij}^{*} \end{aligned}\right\} \quad \text{and} \tag{30}$$

Again, for purposes of the present analysis, it must be noted that in Equation (29), $N_x = 0$ when bending problems are being considered and $p = 0$ when axial compression buckling problems are being considered.

GOVERNING EQUATIONS AND BOUNDARY CONDITIONS FOR LAMINATED FLAT ($R \to \infty$) AND CURVED PLATES

Extremization of the total potential energy functional given by Equation (29) with respect to w, $\vec{u}^{*}$ and $\vec{v}^{*}$ results in the following equilibrium equations and associated boundary conditions. The details of the application of the potential energy principle are given in Appendix III.

Euler Equations

$$\begin{aligned} & t\,\vec{I}^{T}\cdot\tilde{C}_{22}\cdot\vec{I}\,\frac{w}{R^2} - \frac{t}{R}\,\vec{K}_{12}^{T}\cdot\frac{\partial\vec{u}^{*}}{\partial x} - \frac{t}{R}\,\vec{K}_{23}^{T}\cdot\left(\frac{\partial\vec{u}^{*}}{\partial y}+\frac{\partial\vec{v}^{*}}{\partial x}\right) \\ & - \frac{t}{R}\,\vec{K}_{22}^{T}\cdot\frac{\partial\vec{v}^{*}}{\partial y} - tG_B(n-1)\left(\frac{\partial^2 w}{\partial x^2}+\frac{\partial^2 w}{\partial y^2}\right) \\ & + G_B\,\vec{B}^{*T}\cdot\left(\frac{\partial\vec{u}^{*}}{\partial x}+\frac{\partial\vec{v}^{*}}{\partial y}\right) + N_x\frac{\partial^2 w}{\partial x^2} - p = 0 \end{aligned} \tag{31}$$

$$
- t\,\tilde{C}^{*}_{11} \cdot \frac{\partial^2 \vec{u}^{\,*}}{\partial x^2} - t\,\tilde{C}^{*}_{33} \cdot \left(\frac{\partial^2 \vec{u}^{\,*}}{\partial y^2} + \frac{\partial^2 \vec{v}^{\,*}}{\partial x \partial y} \right)
$$

$$
- t\,\tilde{C}^{*}_{12} \cdot \frac{\partial^2 \vec{v}^{\,*}}{\partial x \partial y} - t\,\tilde{C}^{*}_{13} \cdot \frac{\partial^2 \vec{v}^{\,*}}{\partial x^2} - 2t\,\tilde{C}^{*}_{13} \cdot \frac{\partial^2 \vec{u}^{\,*}}{\partial x \partial y}
$$

$$
- t\,\tilde{C}^{*}_{23} \cdot \frac{\partial^2 \vec{v}^{\,*}}{\partial y^2} - G_B \frac{\partial w}{\partial x} \vec{B}^{\,*} + \frac{G_B}{t} \tilde{A}^{*} \cdot \vec{u}^{\,*}
$$

$$
+ \frac{t}{R} \frac{\partial w}{\partial x} \vec{K}_{12} + \frac{t}{R} \frac{\partial w}{\partial y} \vec{K}_{23} = 0 \qquad (32)
$$

$$
- t\,\tilde{C}^{*}_{22} \cdot \frac{\partial^2 \vec{v}^{\,*}}{\partial y^2} - t\,\tilde{C}^{*}_{33} \cdot \left(\frac{\partial^2 \vec{v}^{\,*}}{\partial x^2} + \frac{\partial^2 \vec{u}^{\,*}}{\partial x \partial y} \right)
$$

$$
- t\,\tilde{C}^{*}_{13} \cdot \frac{\partial^2 \vec{u}^{\,*}}{\partial x^2} - t\,\tilde{C}^{*}_{12} \cdot \frac{\partial^2 \vec{u}^{\,*}}{\partial x \partial y} - t\,\tilde{C}^{*}_{23} \cdot \frac{\partial^2 \vec{u}^{\,*}}{\partial y^2}
$$

$$
- 2t\,\tilde{C}^{*}_{23} \cdot \frac{\partial^2 \vec{v}^{\,*}}{\partial x \partial y} - G_B \frac{\partial w}{\partial y} \vec{B}^{\,*} + \frac{G_B}{t} \tilde{A}^{*} \cdot \vec{v}^{\,*}
$$

$$
+ \frac{t}{R} \frac{\partial w}{\partial x} \vec{K}_{23} + \frac{t}{R} \frac{\partial w}{\partial y} \vec{K}_{22} = 0 \qquad (33)
$$

Equations (31), (32) and (33) are the governing equations, expressed in terms of generalized displacements, corresponding to equilibrium in the directions of the displacement w and the generalized displacement vectors $\vec{u}^{\,*}$ and $\vec{v}^{\,*}$, respectively. For application to bending problems, N_x is set equal to zero in Equation (31), whereas for the eigenvalue problem of axial compression buckling, p is set equal to zero.

Boundary Conditions

At $x = 0,L$

$$\left\{ G_B \left[t\,(n-1) \frac{\partial w}{\partial x} - \vec{B}^{*T} \cdot \vec{u}^{*} \right] - N_x \frac{\partial w}{\partial x} \right\} \delta w = 0 \qquad (34)$$

At $y = 0,b$

$$G_B \left[t\,(n-1) \frac{\partial w}{\partial y} - \vec{B}^{*T} \cdot \vec{v}^{*} \right] \delta w = 0 \qquad (35)$$

At $x = 0,L$

$$t \left[\tilde{\tilde{C}}^{*}_{11} \cdot \frac{\partial \vec{u}^{*}}{\partial x} + \tilde{\tilde{C}}^{*}_{12} \cdot \frac{\partial \vec{v}^{*}}{\partial y} + \tilde{\tilde{C}}^{*}_{13} \left(\frac{\partial \vec{v}^{*}}{\partial x} + \frac{\partial \vec{u}^{*}}{\partial y} \right) - \frac{w}{R} \vec{K}_{12} \right] \cdot \delta \vec{u}^{*T} = 0 \qquad (36)$$

At $y = 0,b$

$$t \left[\tilde{\tilde{C}}^{*}_{33} \cdot \left(\frac{\partial \vec{u}^{*}}{\partial y} + \frac{\partial \vec{v}^{*}}{\partial x} \right) + \tilde{\tilde{C}}^{*}_{13} \cdot \frac{\partial \vec{u}^{*}}{\partial x} + \tilde{\tilde{C}}^{*}_{23} \cdot \frac{\partial \vec{v}^{*}}{\partial y} - \frac{w}{R} \vec{K}_{23} \right] \cdot \delta \vec{u}^{*T} = 0 \qquad (37)$$

At $y = 0,b$

$$t \left[\tilde{\tilde{C}}^{*}_{22} \cdot \frac{\partial \vec{v}^{*}}{\partial y} + \tilde{\tilde{C}}^{*}_{12} \cdot \frac{\partial \vec{u}^{*}}{\partial x} + \tilde{\tilde{C}}^{*}_{23} \left(\frac{\partial \vec{u}^{*}}{\partial y} + \frac{\partial \vec{v}^{*}}{\partial x} \right) - \frac{w}{R} \vec{K}_{22} \right] \cdot \delta \vec{v}^{*T} = 0 \qquad (38)$$

At $x = 0,L$

$$t\left[\tilde{C}^{*}_{33}\cdot\left(\frac{\partial\vec{v}^{\,*}}{\partial x}+\frac{\partial\vec{u}^{\,*}}{\partial y}\right)+\tilde{C}^{*}_{23}\cdot\frac{\partial\vec{v}^{\,*}}{\partial y}+\tilde{C}^{*}_{13}\cdot\frac{\partial\vec{u}^{\,*}}{\partial x}-\frac{w}{R}\vec{K}_{23}\right]\cdot\delta\vec{v}^{\,*T}=0 \qquad (39)$$

Equations (34) and (35) require that either the transverse shearing force or the lateral displacement vanishes at the plate edges. Equations (36) and (37) require that either the generalized, axial force vector or the generalized displacement vector in the direction of the axial force vector vanishes at the plate edges. Finally, Equations (38) and (39) require that either the generalized shearing force vector or the generalized displacement vector in the direction of shearing force vector vanishes at the plate edges.

In viewing the boundary conditions, Equations (34) through (39), it can be seen that, unlike conventional plate or shell boundary conditions, there is no condition at any edge corresponding to either arbitrary moments or arbitrary rotations. The mathematical model is such that the bending moment at an edge is represented by the couple of direct stresses acting through the n laminae. Thus, the bending effect appears indirectly in the boundary conditions given by Equations (36) and (38). For example, in the case of simple support there should be no resultant bending moment formed by the laminae membrane stresses at the edges.

The governing equations and boundary conditions given by Equations (31) through (33) and (34) through (39), respectively, have been developed for laminated, composite, anisotropic plate structures characterized by a matrix of finite transverse shear rigidity reinforced by high-strength fibers. For application to the case of plates with interlaminar shear effects neglected, the governing equations and boundary conditions should be used under the condition that $G_B \to E_{11}$. The specialized kinematics of the problem preclude the case $G_B \to \infty$ unless Equations (31) through (33) are coupled by linear operators into a single governing partial differential equation

(of fourth order for plates and eighth order for shells) and, concomitantly, the boundary conditions, Equations (34) through (39), are suitably reduced.

METHOD OF SOLUTION

For problems wherein the plate or shell properties are orthotropic, with the natural and coordinate axes coinciding, the vector and matrices $\vec{K}_{23}$, $\tilde{C}^*_{13}$ and $\tilde{C}^*_{23}$ vanish in both the governing equations and boundary conditions. Consequently, for either a uniform, compressive edge loading or a sinusoidally distributed surface loading acting on a flat or curved plate with classical simple-support boundary conditions, the displacement functions

$$\left.\begin{aligned} \vec{u}^* &= \vec{e}_{ij} \cos \frac{i\pi x}{L} \sin \frac{j\pi y}{b} \\ \vec{v}^* &= \vec{f}_{ij} \sin \frac{i\pi x}{L} \cos \frac{j\pi y}{b} \\ w &= g_{ij} \sin \frac{i\pi x}{L} \sin \frac{j\pi y}{b} \end{aligned}\right\} \qquad (40)$$

satisfy automatically the governing equations and boundary conditions. Substitution of Equations (40) into Equations (31) through (33) leads to a system of algebraic equations which may be solved for either bending ($N_x = 0$) or buckling ($p = 0$) problems, as appropriate.

For laminae in which the natural and coordinate axes do not coincide (anisotropic media), the vector and matrices $\vec{K}_{23}$, $\tilde{C}^*_{13}$, and $\tilde{C}^*_{23}$ do not vanish; thus, the complexity of the equilibrium equations precludes a straightforward solution, even with the usually convenient assumption of simple-support boundary conditions. Solutions for this class of problems are obtained by applying the direct method of the calculus of variations to the total potential energy functional (Rayleigh-Ritz procedure). The minimizing sequences are taken as

$$\left.\begin{aligned} \vec{u}^{\,*} &= \sum_{j=1}^{4} \vec{f}_j \cos\frac{j\pi x}{L} \sin\frac{j\pi y}{b} \\ \vec{v}^{\,*} &= \sum_{j=1}^{4} \vec{f}_j \sin\frac{j\pi x}{L} \cos\frac{j\pi y}{b} \\ w &= \sum_{j=1}^{4} g_j \sin\frac{j\pi x}{L} \sin\frac{j\pi y}{b} \end{aligned}\right\} \qquad (41)$$

where each term of the sequence for w satisfies the geometric boundary conditions of classical, simple support. Details of the procedure for solving the problems of bending and buckling of anisotropic flat plates are given in Appendix IV.

Equations (40) are used in conjunction with Equations (31) through (33) to effect solutions for the bending of simply supported, square, composite plates with orthotropic laminae subjected to the loading $p = p_0 \sin\frac{\pi x}{L} \sin\frac{\pi y}{L}$. Solutions are obtained corresponding to several values of the parameter m in Equation (24), and the results are displayed in Figure 3. Equations (41) are used in conjunction with Equation (29) to obtain solutions for square, flat plates with anisotropic laminae subjected to either a uniformly distributed surface loading or a uniform, compressive loading in the axial direction (see Figure 2); the results are given in Figures 4 through 9. Equations (40) and (31) through (33) are used again to obtain solutions for the buckling of infinitely long, flat and circularly curved plates subjected to a uniform compressive loading in the axial direction (see Figure 2), and the results are presented in Figures 10, 11, and 12.

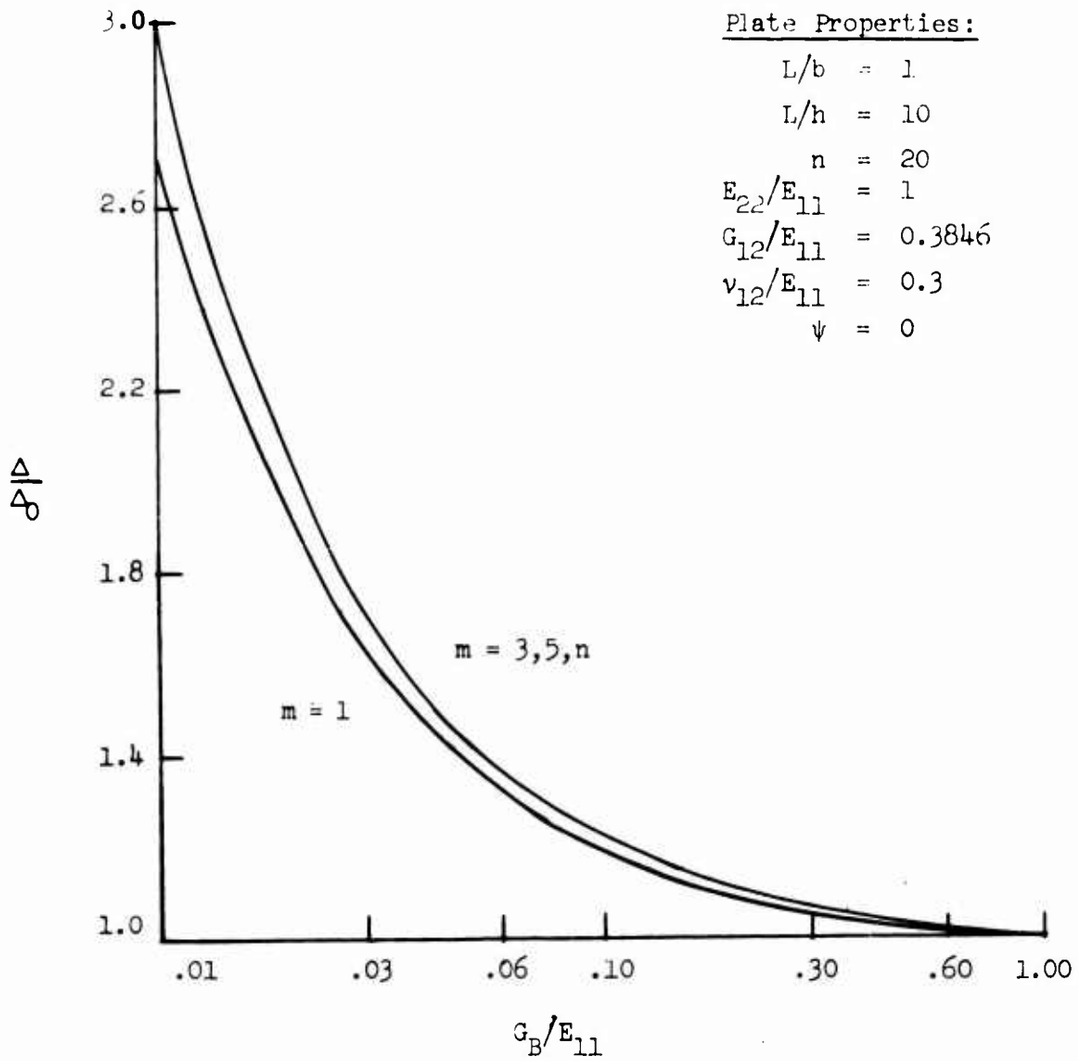

Figure 3. Flat Plate Maximum Deflections Corresponding to Various Approximations to Thickness Distributions of u_k and v_k.

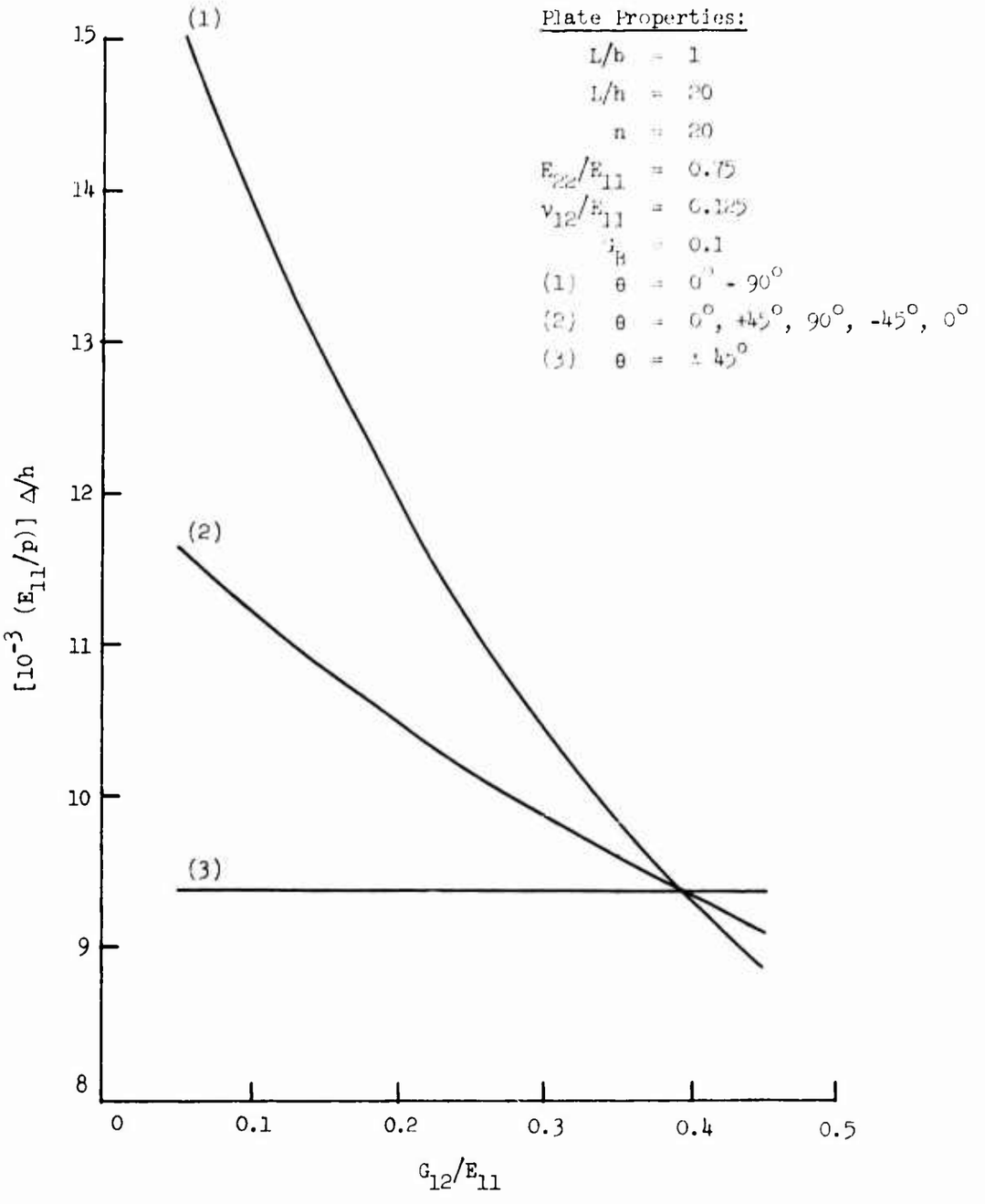

Figure 4. Effects of Parameter G_{12}/E_{11} on Maximum Deflections of Uniformly Loaded Flat Plates.

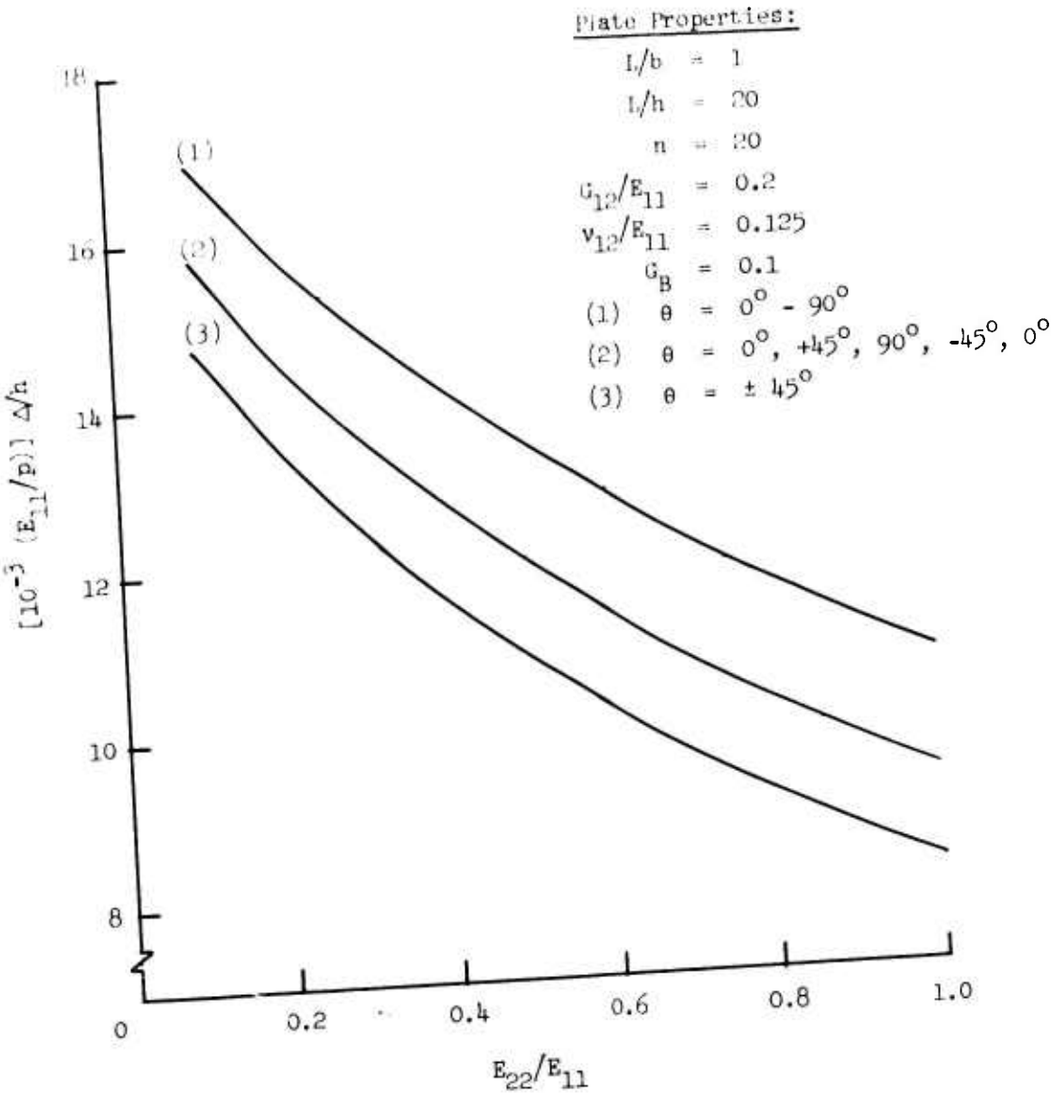

Figure 5. Effects of Parameter E_{22}/E_{11} on Maximum Deflections of Uniformly Loaded Flat Plates.

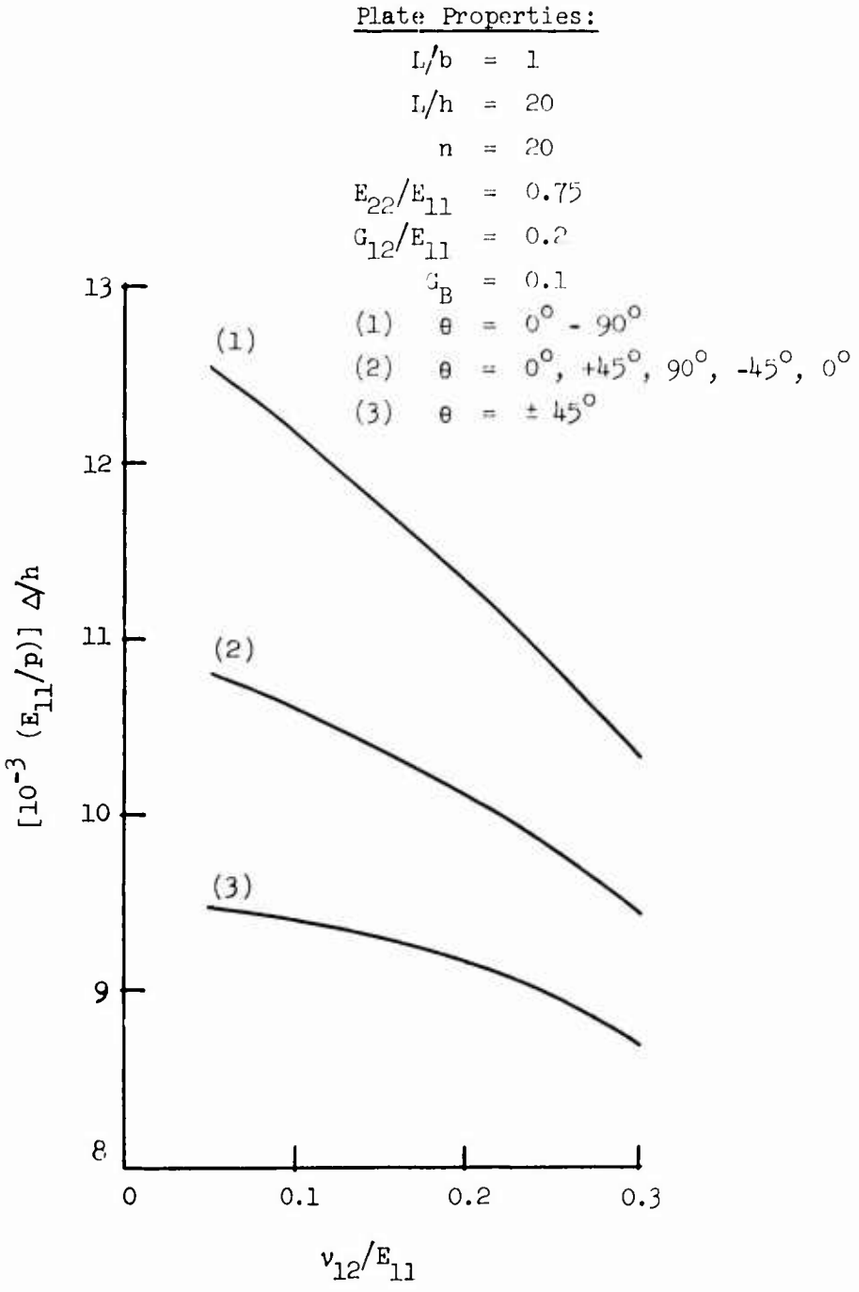

Figure 6. Effects of Parameter ν_{12}/E_{11} on Maximum Deflections of Uniformly Loaded Flat Plates.

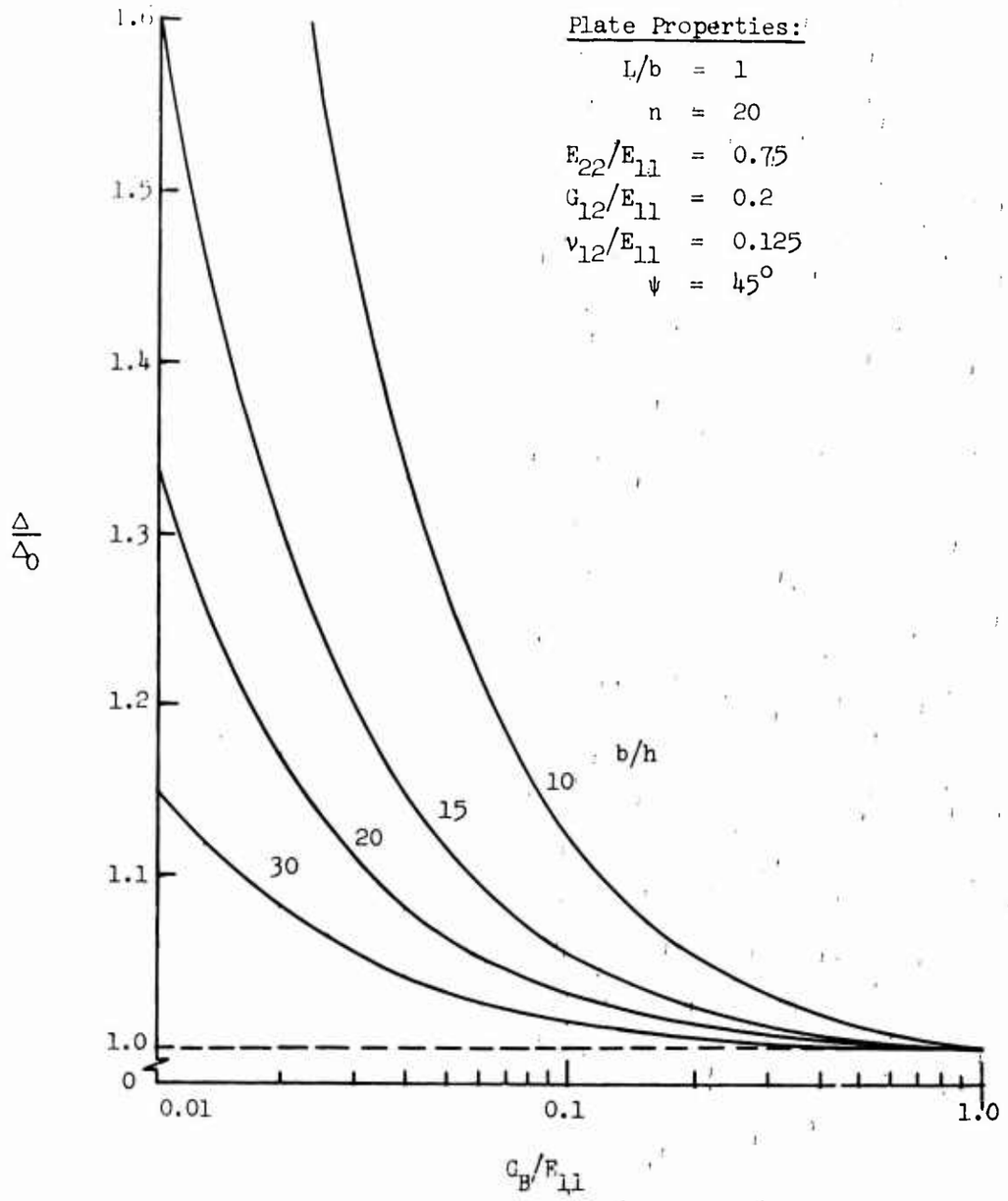

Figure 7. Effects of Interlaminar Shear on Maximum Deflections of Uniformly Loaded Flat Plates.

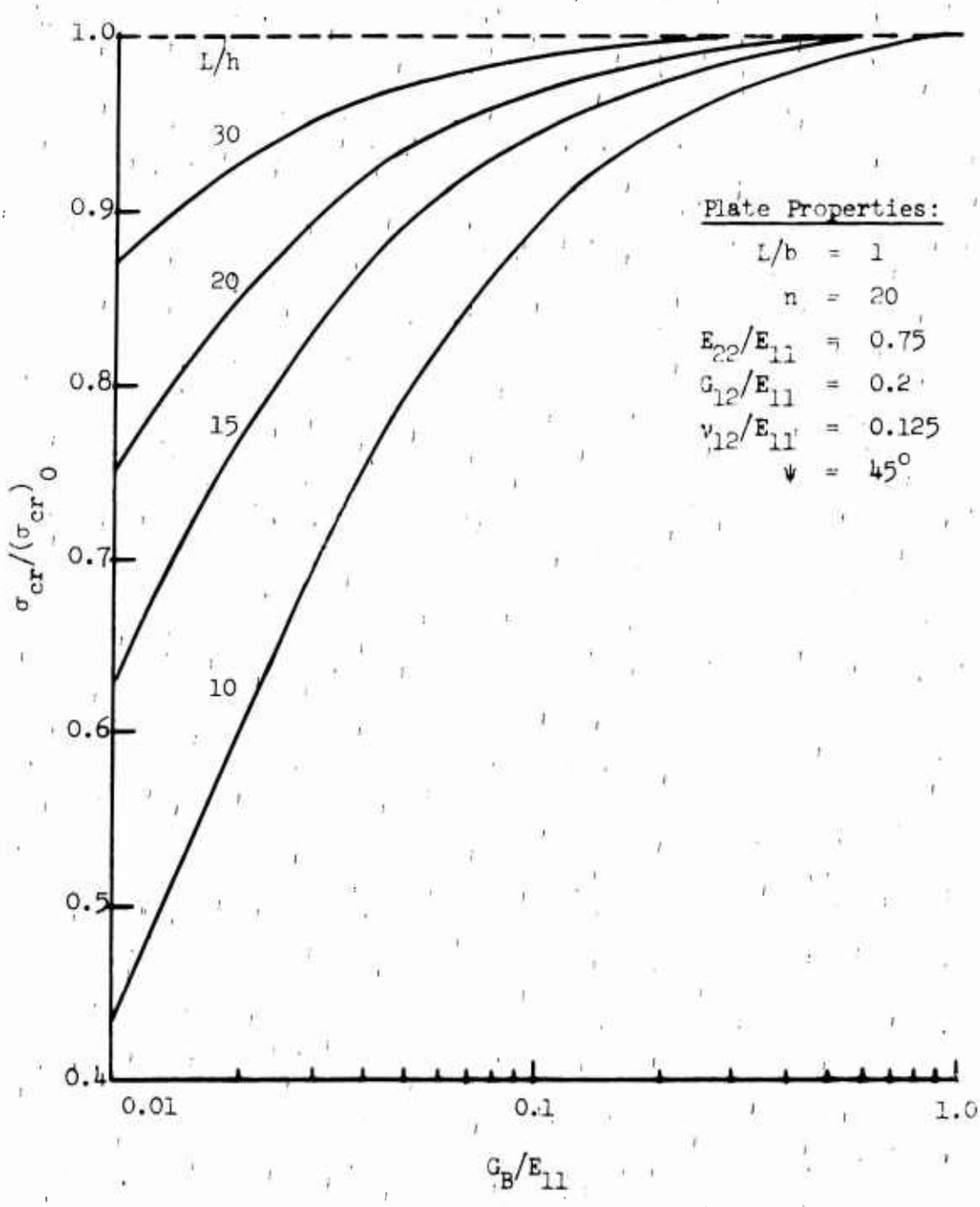

Figure 8. Effects of Interlaminar Shear on Axial Compression Buckling of Flat Plates.

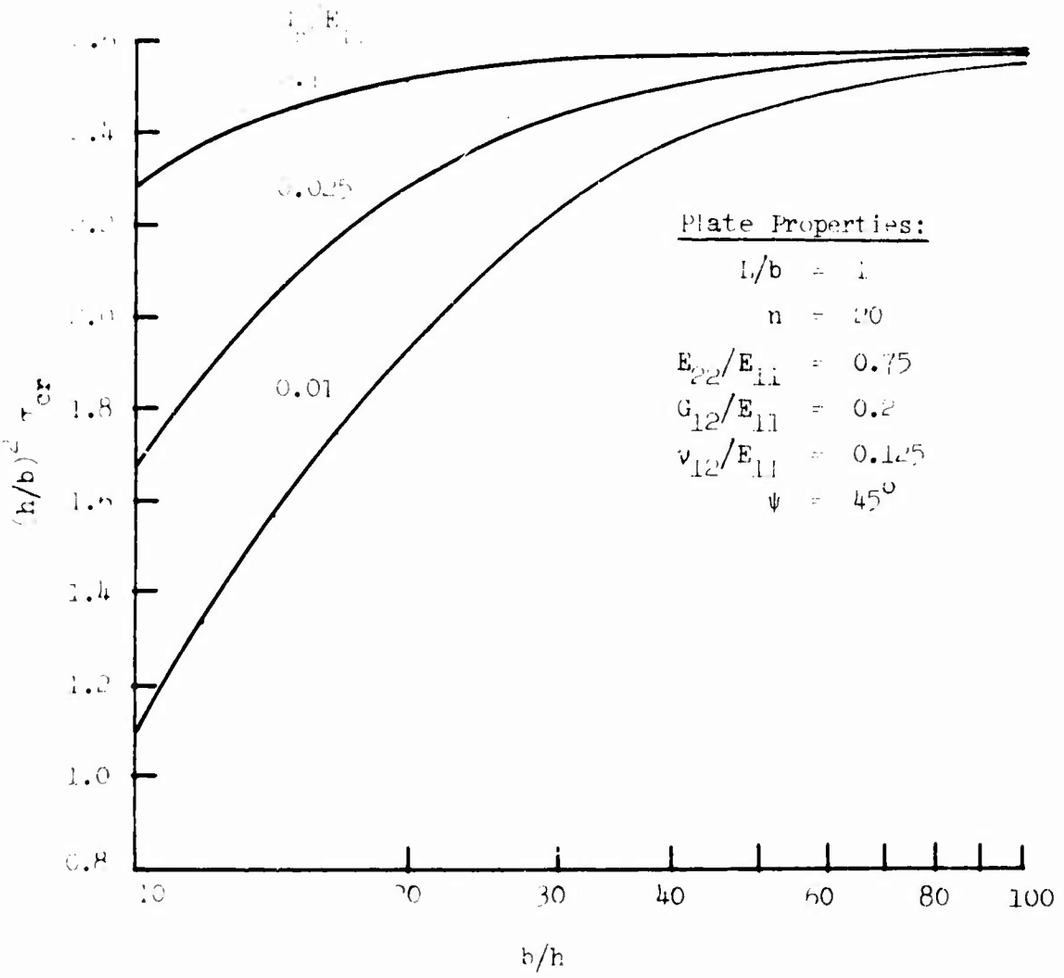

Figure 9. Effects of Interlaminar Shear on Axial Compression Buckling of Flat Plates.

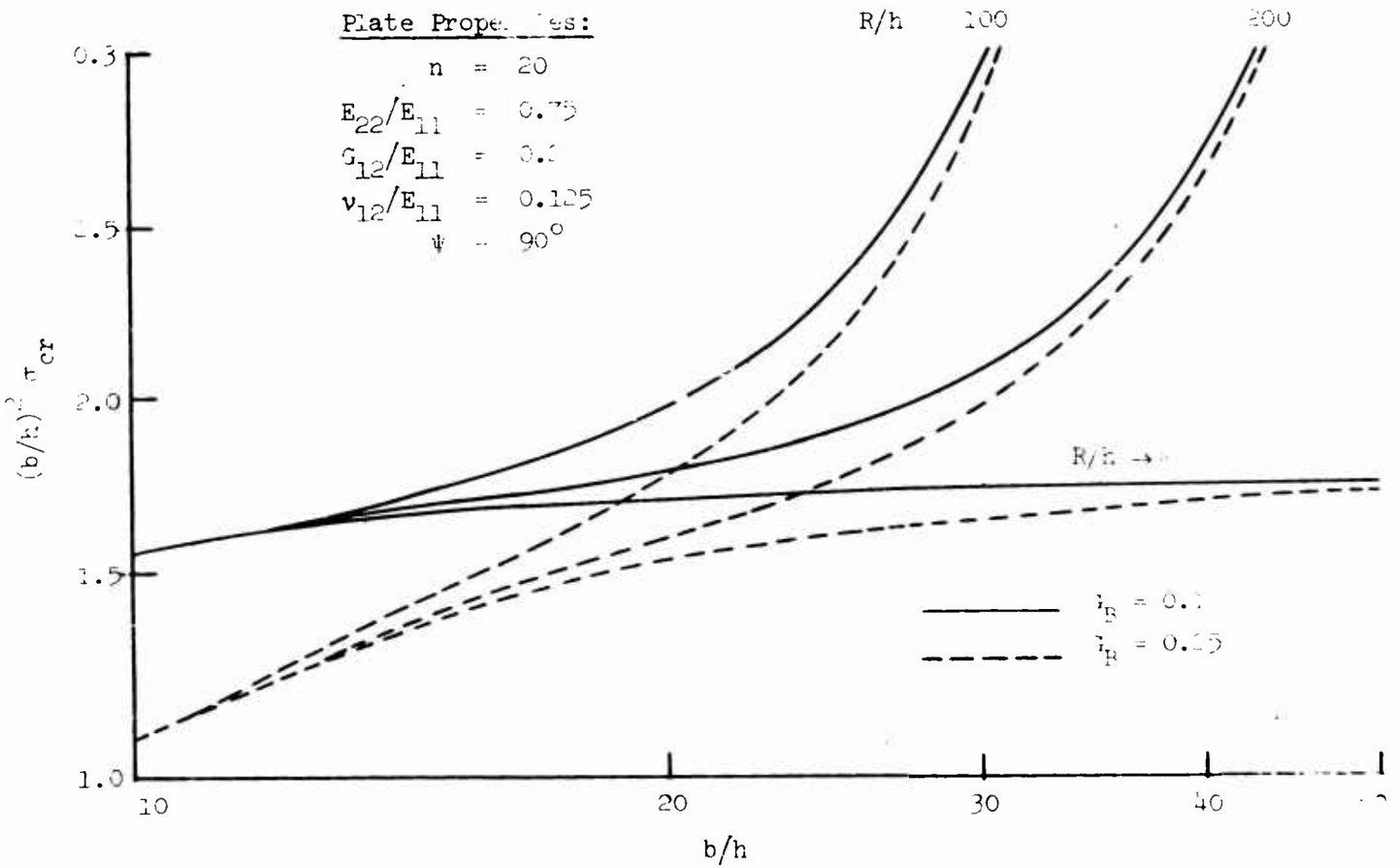

Figure 10. Effects of Interlaminar Shear on Axial Compression Buckling of Long, Circularly Curved, Cylindrical Plates.

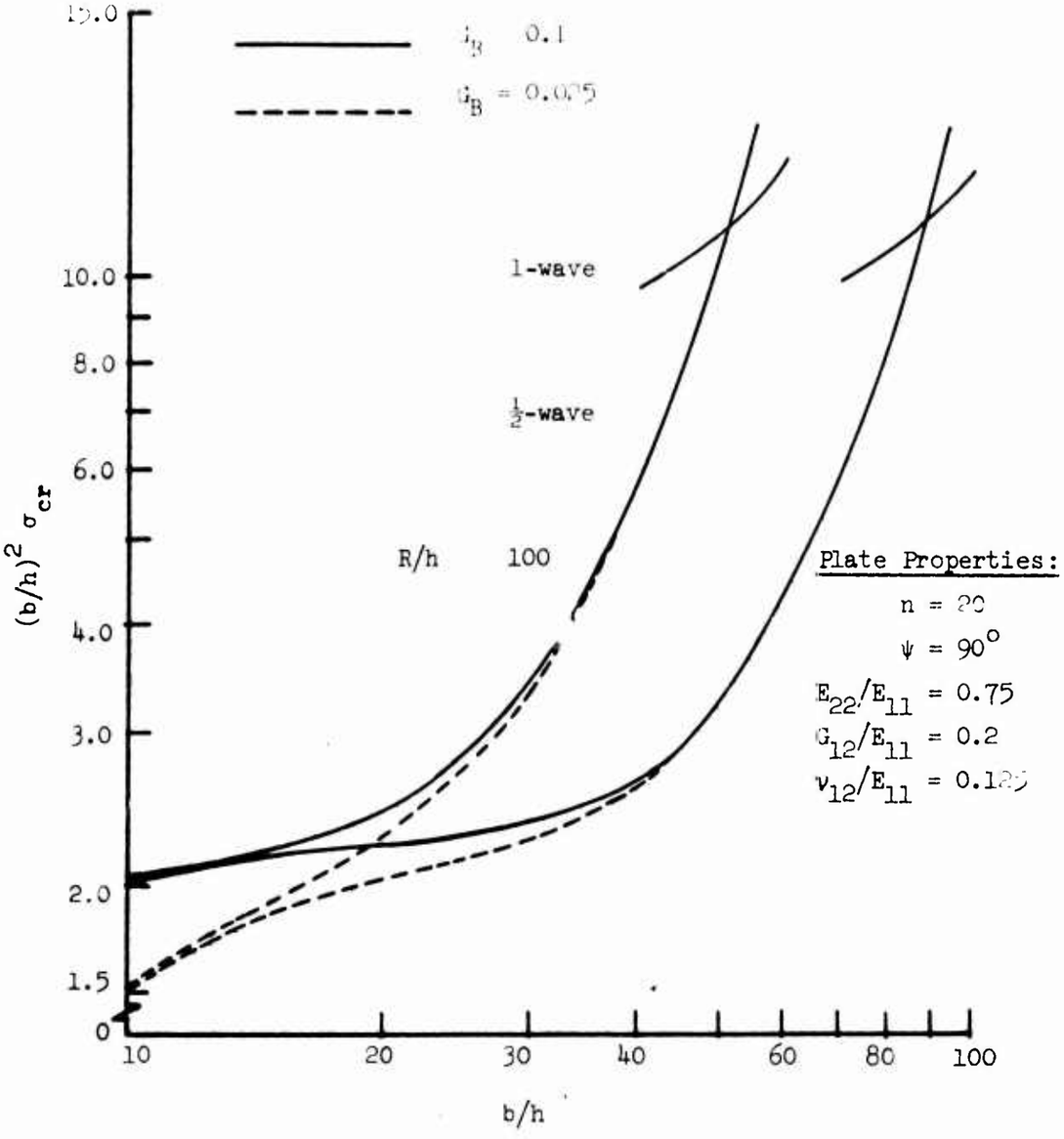

Figure 11. Effects of Interlaminar Shear on Axial Compression Buckling of Long, Circularly Curved, Cylindrical Plates.

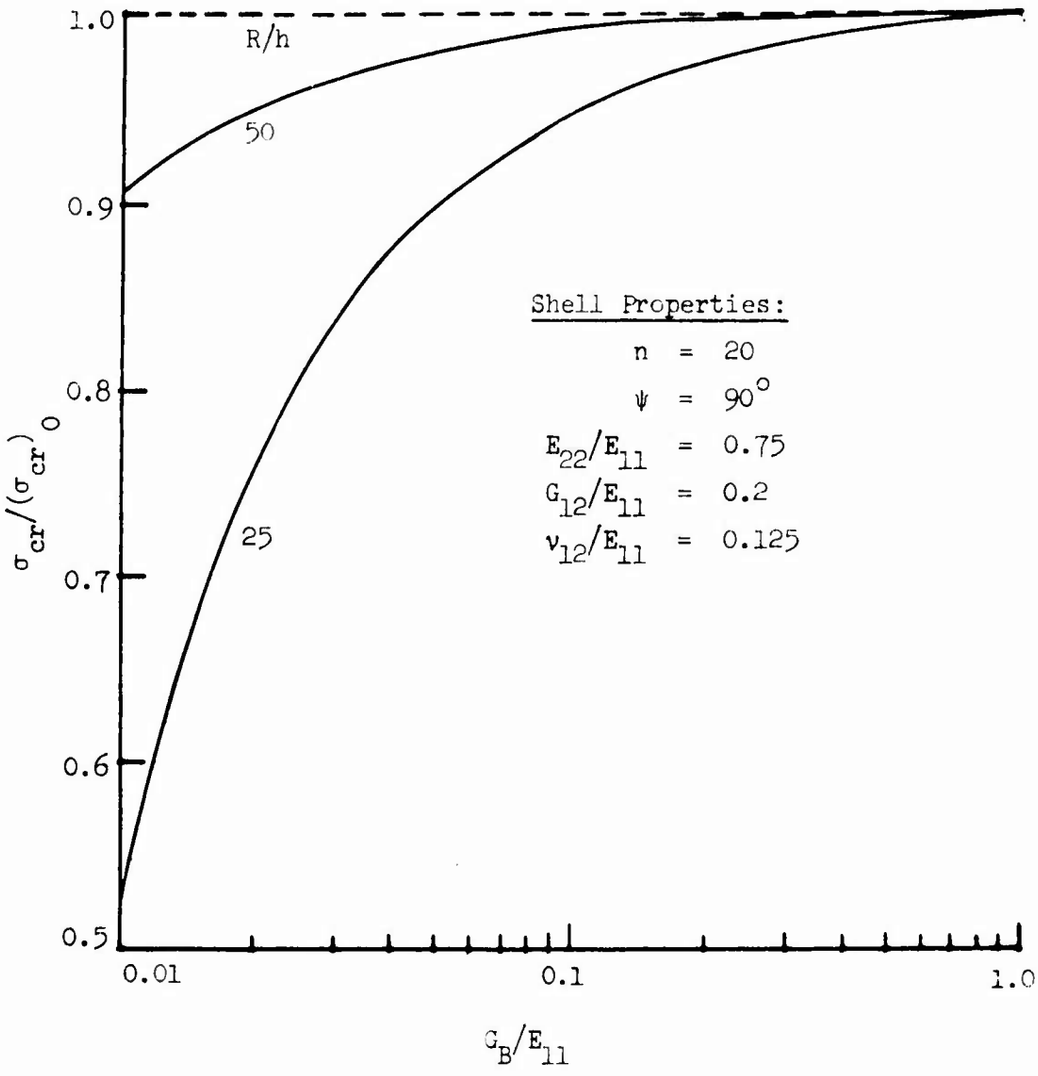

Figure 12. Effects of Interlaminar Shear on Axial Compression Buckling of Long, Thick, Circularly Curved, Cylindrical Shells.

RESULTS AND DISCUSSION

The theory developed in this study is intended for application to laminated plates and shells. However, the equations presented can be modified easily and applied to a much wider class of problems. In the development, plates and shells are considered to be composed of a number of thin laminae; however, there is no requirement that there be a one-to-one relationship between the laminae in the actual structure and those of the analytical model. Thus, the complex behavior of, for example, conventionally thick plates and multilayered sandwich constructions can be approximated by representing the structures as laminates. Individual lamina can be assigned properties appropriate to the physical description of the actual structure. The kinematics of the laminae provide automatically for transverse shear deformations. Then, by introducing independence of the lateral displacements of each lamina, the effects of both transverse shear and normal strain can be taken into account. Ordinarily, such modeling would imply extensive, if not prohibitive, computations. However, by the introduction of the vector-matrix techniques used in this study, the apparent tediousness of analysis can be greatly reduced.

APPLICATION TO LAMINATED, COMPOSITE FLAT AND CURVED PLATES

Validity of "Plane Sections" Assumption

The degree of approximation of the displacement vectors is determined by the number of columns in the matrix $\tilde{Q}$ appearing in Equations (20) and (21) and given by Equation (24). In the latter equation, the number of columns in $\tilde{Q}$ is indicated as $m + 1$, where m is left arbitrary. The effect of the matrix Q on the analysis is to impose a constraint on the distortion of a transverse cross section. If m were set equal to unity, cross sections would be constrained to remain plane (but not normal) after deformation. Higher values of m allow cross sections to distort into shapes described by higher degree polynomials.

The choice of a suitable value of m for use in the analyses undertaken herein is based on the results presented in Figure 3. There, the curves show the effects of the shear stiffness parameter, G_B/E_{11}, on the deflections of a laterally loaded, simply supported, square plate as given by solutions corresponding to various values of m. The ordinates in Figure 3 are the maximum, normalized deflections, with normalization carried out with respect to the deflections of a similar plate having infinite transverse shear rigidity. The plate properties are indicated in the figure; these properties tend to maximize the effects of transverse shear in plate-type structures. The plate loading is of the type $p = p_0 \sin \frac{\pi x}{L} \sin \frac{\pi y}{b}$.

Solutions corresponding to three values of m in Equation (24) are shown in Figure 3. In addition, the solution corresponding to the case in which no approximation is introduced is shown and labeled $m = n$. The curves of Figure 3 illustrate that only a small increase in accuracy is obtained by changing from $m = 1$ to $m = 3$, and that no appreciable increase in accuracy is obtained in taking $m > 3$. In all, the assumption of transverse cross sections remaining plane, implied in using $m = 1$, results in a good approximation of the effects of interlaminar shear for the parameters given in Figure 3. Thus, at least on the basis of the results obtained here, the assumption of plane sections remaining plane but not normal used in Reference 9 appears to be valid. The same assumption (corresponding to $m = 1$) is the basis of all subsequent calculations presented in this study. The governing equations and boundary conditions for flat plates, Equations (31) through (39), are expanded into scalar form for the case $m = 1$ and are shown to reduce to the Reissner plate theory for homogeneous plates with the effects of transverse shear included.[17]

Coupling Between Bending and Membrane Stresses

The coupling between bending and membrane stresses noted in References 2 through 4 is present in this analysis in the form of coupling between coefficients of the even and odd powers of z (see Equation 24). The terms involving even powers of z correspond to extensional displacements,

whereas terms involving odd powers of z correspond to bending displacements.[18] In the case of structures which are symmetric about a median surface and have the reference surface ($z = 0$) coinciding with this median surface, the even-powered terms in Equation (24) can have no net effect on the results. For laminates symmetric about a median surface, but having the reference surface ($z = 0$) at any other location, the even- and odd-powered terms couple in any solution. This is the case with the problem results presented in Figure 3 where the reference surface has been taken at the median surface of the extreme lamina. For nonsymmetric laminates (all other cases considered in this section), coupling is always present unless a neutral surface can be identified readily and the reference surface located thereon. In the present vector-matrix approach, no special consideration need be given the question of coupling between membrane and bending stresses as the operations involved, unlike the more conventional techniques (see, for example, References 2, 3, and 4), introduce no additional complexity in that they adjust automatically for any choice of reference surface location.

Effects of Parameters G_{12}/E_{11}, E_{22}/E_{11}, and ν_{12}/E_{11} on Bending of Plates Under Lateral Loading

The effects of variations in the parameters G_{12}/E_{11}, E_{22}/E_{11}, and ν_{12}/E_{11} on the maximum deflections of a uniformly loaded, square composite plate have been studied, and the results are presented in Figures 4 through 6. In each figure, curves corresponding to three different fiber orientations are shown. Curve (1) in each case corresponds to a construction in which the fibers are aligned parallel to the plate edges and change orientation by 90° increments between adjacent laminae. Curve (2) corresponds to a construction in which the fibers are alternately aligned parallel to the plate edges and the plate diagonals; thus, the fibers change orientation by 45° between adjacent laminae. Curve (3) corresponds to a construction in which the fibers are always aligned along the plate diagonals and change orientation by 90° between adjacent laminae. The other properties are as indicated in the figures.

Figure 4 displays the effect of variations in G_{12}/E_{11} on maximum plate deflections and shows that when the fibers are oriented along the plate diagonals in a square plate, the magnitude of G_{12} has no effect on the deflections. This is the same phenomenon noted by Reissner and Stavsky[2] in considering a Smith-type plate wherein the angle between the natural and coordinate axes was 45°. The explanation is that for a uniformly loaded, square plate, the directions of the principal stresses are parallel to the diagonals; hence, when the fibers are parallel to the diagonals, the laminae transmit no shearing stress and the shear modulus has no effect. For the other two types of construction, Figure 4 shows the ratio of laminae shear to extensional moduli to have a considerable effect on the plate behavior. It is evident that constructions of type (1) are particularly poor choices for composites having low ratios of G_{12}/E_{11}. For composites constructed in the manner of type (1), this effect can diminish the potential advantage in using very high strength fibers. It is interesting to note that at approximately $G_{12}/E_{11} = 0.4$ the relative rigidities of the constructions reverse. For ratios higher than 0.4 the ability of the laminae to resist inplane shear exceeds its ability to resist extension and, hence, the most favorable construction is that wherein relatively high shearing stresses can be induced.

The essentially parallel nature of the curves in Figures 5 and 6 indicates that while the ratios E_{22}/E_{11} and ν_{12}/E_{11} do, of course, have an effect on the bending rigidity, this effect is only slightly influenced by the type of construction. The differences in deflections obtained for the three types of construction in Figures 5 and 6 can be attributed, in accordance with Figure 4, to the effect of $G_{12}/E_{11} = 0.2$.

Effects of Interlaminar Shear on the Bending and Buckling of Flat Plates

The effects of interlaminar shear on the bending and buckling of composite flat plates are illustrated by considering the behavior of square, simply supported plates of varying aspect ratio subjected to either a uniformly distributed surface loading or a uniform axial compression loading. Results, normalized with respect to the behavior of similar

plates having the shear stiffness parameter $G_B/E_{11} \to 1$, are given in Figures 7 and 8 for the bending and buckling problems, respectively. Other physical constants for the plates analyzed are as indicated in the figures.

Representative values for G_B/E_{11} are 0.1 (glass epoxy) and 0.025 (boron-epoxy). This range should be representative also of some of the newer plastic composites under consideration which utilize graphite, silicon carbide, and beryllium fibers as the reinforcing elements. For relatively thin plates, $b/h > 30$, the bending and buckling are significantly influenced by interlaminar shear effects when the shear stiffness parameter is in the range $G_B/E_{11} < 0.04$. On the other hand, for relatively thicker plates, say, $b/h < 15$, the effects of interlaminar shear are significant when $G_B/E_{11} < 0.1$. Of importance is the fact that for composite plates in the initial portion of the thin plate range and $G_B/E_{11} < 0.025$, small reductions in the shear stiffness parameter produce large increases in plate shear flexibility. Thus, in the bending and buckling analyses of practical thin plates and plate elements in, say, stiffeners made of very high-strength-fiber composites, such as boron-epoxy, interlaminar shear effects should not be overlooked.

Design data for composite plates with properties other than those used to obtain the results presented in Figures 7 and 8 can be derived from charts similar to Figures 4, 5, 6, and 9. Charts such as Figure 9 could be used to first determine, for example, the buckling stress corresponding to prescribed values of b/h and G_B/E_{11} and a reference set of laminae parameters $(G_{12}/E_{11}$, E_{22}/E_{11} , $\nu_{12}/E_{11})$. Then, adjustment for the actual laminae parameters could be made by use of charts similar to Figures 4 through 6.

Effects of Interlaminar Shear on the Buckling of Curved Plates and Shells Under Axial Compression

The effects of interlaminar shear on the axial compression buckling of long, thin, circularly cylindrical composite plates and shells having classical simple-support boundary conditions are illustrated by

considering the behavior of plates having specific R/h and G_B/E_{11} values and varying cross-section aspect ratios. The results are presented in Figures 10 and 11. Figure 10 indicates that the presence of shallow curvature does not significantly modify the effects of interlaminar shear obtained for the buckling of flat plates $(R \to \infty)$. For such curvature, the long plate develops only rectangular buckles along its length (one buckle half-wavelength in the circumferential direction), the buckle configuration obtained in the case of flat plates.

In Figure 11, the same parameters as those used to develop Figure 10 are reused; however, a longer ordinate range is shown. The results now indicate that as the curved plate cross-section aspect ratio, b/h , approaches the value at which the plate behaves as a shell (shell behavior being characterized by a buckled configuration of two or more half-waves in the circumferential direction), the effects of interlaminar shear become negligible. This result means simply that the range of thin shell behavior, wherein transverse shear effects are quite small, has been reached. When thicker shells are considered, as in Figure 12, interlaminar shear, as would be expected, is seen to have a considerable effect. In this figure the critical axial compressive stress has been normalized with respect to that of similar shells having a shear stiffness parameter value $G_B/E_{11} \to 1$. The conclusion regarding the small effect of interlaminar shear in thin composite shells corroborates the results given in Reference 10. Therein, Taylor and Mayers, on the basis of a first-approximation theory, studied the effects of interlaminar shear on the axial compression buckling of thin boron-epoxy and glass-epoxy cylindrical shells; they concluded that interlaminar shear effects could be neglected for thin composite shells using current high-performance fibers.

CONCLUDING REMARKS

A small deflection theory has been developed to assess the effects of interlaminar shear on the bending and buckling of flat and circularly curved plates of composite construction. The theoretical developments, in the form of governing equations and associated boundary conditions, are sufficiently general to encompass anisotropic, circularly curved, cylindrical plate elements of nonsymmetric cross section. Specific applications have been made to the bending and the axial compression buckling of simply supported flat plates and to the axial compression buckling of curved plates and shells having classical, simple supports.

In the cases investigated, the interlaminar shear effects in composite plates having moderate cross section aspect ratios, say, $15 < \frac{b}{h} < 30$, become significant when the shear stiffness parameter, G_B/E_{11}, is less than about 0.04 . For relatively thicker plates, however, the interlaminar shear effects become significant when the shear stiffness parameter is less than about 0.1 . In the case of thin, highly curved plates and shells, the results indicate that the interlaminar shear effects are negligible when the shear stiffness parameter exceeds about 0.01 . For practical composite plates and shells of, for example, boron- or glass-epoxy construction, effects of interlaminar shear are shown to be adequately described by a first approximation theory as that used in Reference 10; such a theory is given by this analysis when the exponent, m, in the power series approximation for distributions through the plate thickness of the inplane displacements is equal to unity. It is shown also that when $m = 1$, the governing equations for flat plates reduce to the theory attributed to Reissner for homogeneous plates with the effects of transverse shear included.

Though well suited for composite constructions, the present theory is not limited to such applications. The theory could be used, for example, to treat the complex behavior of conventional thick plates and multilayered sandwich constructions (for example, normal strain and transverse shear effects in heated plates with irregular thermal gradients through the

thickness). When solutions are obtained with the aid of high speed computers, the vector-matrix development used in the present analysis affords more than a notational advantage as the necessary operations (obviously tedious for a fully coupled, anisotropic plate problem) can be performed by the computer and, hence, they need not be expanded. Further, the approximations to the displacement vectors introduced effect a considerable reduction in the computer time required to obtain solutions. For example, the time required to solve the governing equations on an IBM 360 computer for a 20-layered plate and m equal to unity is less than 3 seconds, whereas the time required to solve the equivalent set of equations with no approximation introduced (m = 20) is more than 30 seconds.

Although the present theory is limited to problems which are kinematically and constitutively linear, the variational development can be extended to include nonlinear strain-displacement relations. Since many fiber composites possess essentially linear stress-strain relationships, the question of nonlinear constitutive laws does not appear at the present time to pose a pressing problem. However, the effect of interlaminar shear on the behavior of composite plates and shells in the large deflection region could be quite significant and should be assessed. The theoretical analysis and method of solution presented herein offers an attractive approach to this problem.

LITERATURE CITED

1. Smith, C. B., SOME NEW TYPES OF ORTHOTROPIC PLATES LAMINATED OF ORTHOTROPIC MATERIAL, Journal of Applied Mechanics, Vol. 20, Trans. ASME, Vol. 75, 1953, pp. 286-288.

2. Reissner, E., and Stavsky, Y., BENDING AND STRETCHING OF CERTAIN TYPES OF HETEROGENEOUS AEOLOTROPIC ELASTIC PLATES, Journal of Applied Mechanics, Vol. 28, No. 3, Trans. ASME, Vol. 83, Series E, September 1961, pp. 402-408.

3. Dong, S. B., Pister, K. S., and Taylor, R. L., ON THE THEORY OF LAMINATED ANISOTROPIC SHELLS AND PLATES, Journal of the Aerospace Sciences, Vol. 29, No. 8, August 1962, pp. 969-975.

4. Whitney, J. M., and Leissa, A. W., ANALYSIS OF HETEROGENEOUS ANISOTROPIC PLATES, Journal of Applied Mechanics, June 1969, pp. 261-266.

5. Donnell, L. H., STABILITY OF THIN-WALLED TUBES UNDER TORSION; NACA TR 479, 1933.

6. Pagano, N. J., ANALYSIS OF THE FLEXURE TEST OF BIDIRECTIONAL COMPOSITES, Journal of Composite Materials, Vol. 1, 1967, pp. 336-342.

7. Whitney, J. M., THE EFFECT OF TRANSVERSE SHEAR DEFORMATION ON THE BENDING OF LAMINATED PLATES, Journal of Composite Materials, Vol. 3, July 1969, pp. 534-547.

8. Ambartsumyan, S. A., THEORY OF ANISOTROPIC SHELLS, NASA TT F-118, 1964.

9. Khot, N. S., ON THE EFFECTS OF FIBER ORIENTATION AND NONHOMOGENEITY ON BUCKLING AND POSTBUCKLING EQUILIBRIUM BEHAVIOR OF FIBER-REINFORCED CYLINDRICAL SHELLS UNDER UNIFORM AXIAL COMPRESSION, AFFDL-TR-68-19, Air Force Flight Dynamics Laboratory, Wright-Patterson Air Force Base, Ohio, 1968.

10. Mayers, J., and Taylor, R. M., A FIRST APPROXIMATION THEORY TO THE EFFECTS OF TRANSVERSE SHEAR DEFORMATIONS ON THE BUCKLING AND VIBRATION OF FIBER-REINFORCED, CIRCULAR CYLINDRICAL SHELLS – APPLICATION TO AXIAL COMPRESSION LOADING OF BORON- AND GLASS-EPOXY COMPOSITES, USAAVLABS Technical Report 70-8, U.S. Army Aviation Materiel Laboratories, Fort Eustis, Virginia, March 1970, AD 871610.

11. Mayers, J., and Nelson, E., MAXIMUM STRENGTH ANALYSIS OF POSTBUCKLED RECTANGULAR PLATES, Presented at AIAA Sixth Aerospace Sciences Meeting, AIAA Paper No. 68-171, New York, January 1968.

12. Libove, C., and Batdorf, S. B., A GENERAL SMALL-DEFLECTION THEORY FOR FLAT SANDWICH PLATES, NACA TN 1526, 1948.

13. Hoff, N. J., BENDING AND BUCKLING OF RECTANGULAR SANDWICH PLATES, NACA Technical Note 2225, November 1950.

14. Benson, A. S., and Mayers, J., GENERAL INSTABILITY AND FREE WRINKLING OF SANDWICH PLATES – UNIFIED THEORY AND APPLICATIONS, AIAA Journal, Vol. 5, No. 4, April 1967, pp. 729-739.

15. Durlofsky, H., and Mayers, J., EFFECTS OF INTERLAMINAR SHEAR ON THE BENDING AND BUCKLING OF LAMINATED BEAMS, USAAVLABS Technical Report 70-7, U.S. Army Aviation Materiel Laboratories, Fort Eustis, Virginia, March 1970, AD 871426.

16. Calcote, L. R., THE ANALYSIS OF LAMINATED COMPOSITE STRUCTURES, Van Nostrand Reinhold Company, 1969.

17. Timoshenko, S., and Woinowsky-Krieger, S., THEORY OF PLATES AND SHELLS, 2nd ed., McGraw-Hill, 1959.

18. Menlin, R. D., AN INTRODUCTION TO THE MATHEMATICAL THEORY OF VIBRATIONS OF ELASTIC PLATES, U.S. Army Signal Corps Monograph, Department of the Army Project 3-99-11-022, 1955.

APPENDIX I

STRAIN ENERGY DUE TO TRANSVERSE SHEAR

For a matrix material with infinite shear rigidity, an element taken from two adjacent laminae (see Figure 13a) distorts due to bending as shown in Figure 13b; the relationship between the inplane and lateral displacement functions is simply

$$\frac{\partial w}{\partial x} = \frac{u_k - u_{k+1}}{t} \tag{42}$$

With finite shear rigidity of the matrix material, the cross section experiences the additional rotation $\gamma_{xz}^{(k)}$ as indicated in Figure 13c. Similar considerations apply to the distortions in the y-z plane. Thus, the relationships between both the inplane and lateral displacement functions and the transverse shearing strains become

$$\left.\begin{aligned} \gamma_{xz}^{(k)} &= \frac{u_k - u_{k+1}}{t} - \frac{\partial w}{\partial x} \\ \gamma_{yz}^{(k)} &= \frac{v_k - v_{k+1}}{t} - \frac{\partial w}{\partial y} \end{aligned}\right\} \tag{43}$$

The strain energy due to transverse shear is

$$U_s = \sum_{k=1}^{n-1} \frac{G_B t}{2} \int_0^L \int_0^b \left\{ \left[\gamma_{xz}^{(k)}\right]^2 + \left[\gamma_{yz}^{(k)}\right]^2 \right\} dxdy \tag{44}$$

Introduction of Equations (43) into Equation (44) gives the final form

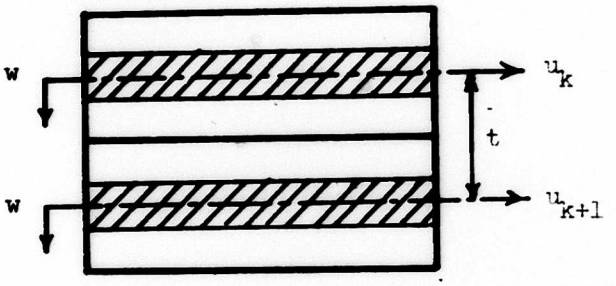

(a) Geometry of Two Adjacent Laminae

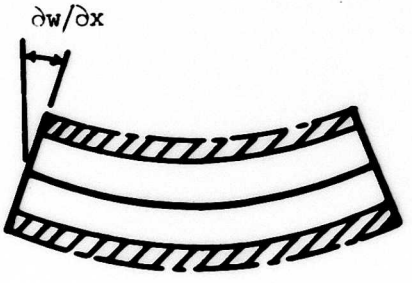

(b) Distortion of Element with $G_B \to \infty$

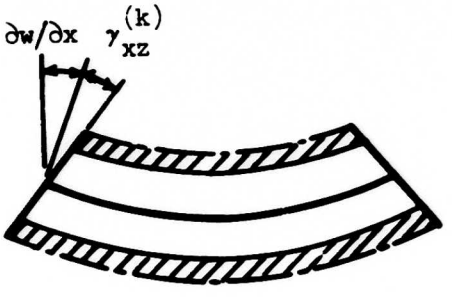

(c) Distortion of Element with $0 < G_B < \infty$

Figure 13. Geometry of Transverse Shear Deformation.

of the strain energy of transverse shear as

$$U_s = \sum_{k=1}^{n-1} \frac{G_B t}{2} \int_0^L \int_0^b \left[\left(\frac{\partial w}{\partial x} - \frac{u_k - u_{k+1}}{t} \right)^2 \right.$$

$$\left. + \left(\frac{\partial w}{\partial y} - \frac{v_k - v_{k+1}}{t} \right)^2 \right] dxdy \qquad (45)$$

APPENDIX II

REDUCTION OF THE NUMBER OF INDEPENDENT INPLANE DISPLACEMENT FUNCTIONS

The displacement functions u_k and v_k, $k = 1,2,\ldots,n$, are all functions of the x and y coordinates only; that is,

$$u_k = u_k(x,y) \qquad k = 1,2,\ldots,n \tag{46}$$

$$v_k = v_k(x,y) \qquad k = 1,2,\ldots,n \tag{47}$$

Due to the continuity of the deformed structure, there exist functions $F_1 = F_1(x,y,z)$ and $F_2 = F_2(x,y,z)$ such that

$$F_1(x,y,z_k) = u_k(x,y) \qquad k = 1,2,\ldots,n \tag{48}$$

$$F_2(x,y,z_k) = v_k(x,y) \qquad k = 1,2,\ldots,n \tag{49}$$

where z_k is the distance from a reference plane to the center of the k^{th} lamina (see Figure 1). The functions F_1 and F_2 can be expanded into a power series in z. These expansions are written as

$$F_1(x,y,z) = u_0^*(x,y) + z\,u_1^*(x,y) + \ldots + z^m u_m^*(x,y) + \ldots \tag{50}$$

$$F_2(x,y,z) = v_0^*(x,y) + z\,v_1^*(x,y) + \ldots + z^m v_m^*(x,y) + \ldots \tag{51}$$

The right-hand sides of Equations (50) and (51) have at most n terms since, corresponding to any location on the reference surface, F_1 and F_2 must pass through n points and, therefore, can be given by a $n-1$ degree polynomial in z.

Approximations of the functions F_1 and F_2 are effected by terminating the expansions given by Equations (50) and (51) with the m^{th} term. Approximation of F_1 in this manner and introduction of the approximation into Equations (48) give

$$\left.\begin{aligned} u_1 &= u_0^* + z_1 u_1^* + \ldots + z_1^m u_m^* \\ u_2 &= u_0^* + z_2 u_1^* + \ldots + z_2^m u_m^* \\ &\vdots \\ u_n &= u_0^* + z_n u_1^* + \ldots + z_n^m u_m^* \end{aligned}\right\} \qquad (52)$$

Equations (52) can be represented in vector-matrix form as

$$\vec{u} = \tilde{Q} \cdot \vec{u}^* \qquad (53)$$

where

$$\vec{u}^* = \begin{Bmatrix} u_0^* \\ u_1^* \\ \vdots \\ u_m^* \end{Bmatrix} \qquad (54)$$

and

$$\tilde{Q} = \begin{vmatrix} 1 & z_1 & z_1^2 & \cdots & z_1^n \\ 1 & z_2 & z_2^2 & \cdots & z_2^n \\ \vdots & & & & \\ 1 & z_m & z_m^2 & \cdots & z_m^n \end{vmatrix} \tag{55}$$

A similar development for $\vec{v}$ results in

$$\vec{v} = \tilde{Q} \cdot \vec{v}^* \tag{56}$$

where

$$\vec{v}^* = \begin{Bmatrix} v_0^* \\ v_1^* \\ \vdots \\ v_m^* \end{Bmatrix} \tag{57}$$

Thus, Equations (53) and (56) represent the transformation of the $2n$ displacement functions u_k and v_k, $k = 1,2,\ldots,n$, into the $2(m + 1)$ generalized displacement functions u_k^* and v_k^*, $k = 1,2,\ldots,m$. The transformation is quite useful in analyzing the behavior of thin, laminated, anisotropic flat and curved plates since, normally, $m \ll n$.

APPENDIX III

VARIATION OF TOTAL POTENTIAL ENERGY

To establish the governing equations of equilibrium and the associated boundary conditions, a stationary value of the total potential energy, Equation (29), is sought with respect to admissible variations in the lateral displacement function w and the generalized inplane displacement vectors $\vec{u}^{\,*}$ and $\vec{v}^{\,*}$. Although the variational process should, in general, be carried out simultaneously with respect to w, $\vec{u}^{\,*}$ and $\vec{v}^{\,*}$, the formulation of the present problem is such that no loss of generality in the derivation is incurred by carrying out the variations separately.

Variation of the total potential energy functional, Equation (29), with respect to the displacement function w gives

$$\delta_w(U + V) = \int_0^L\int_0^b \left\{ -\frac{t}{R}\left[\vec{K}_{12}^{T} \cdot \frac{\partial \vec{u}^{\,*}}{\partial x} + \vec{K}_{23}^{T} \cdot \frac{\partial \vec{v}^{\,*}}{\partial x} + \vec{K}_{23}^{T} \cdot \frac{\partial \vec{u}^{\,*}}{\partial y} + \vec{K}_{22}^{T} \cdot \frac{\partial \vec{v}^{\,*}}{\partial y}\right] + \frac{tw}{R^2}\, \vec{I}^{\,T} \cdot \tilde{C}_{22} \cdot \vec{I} \right\} \delta w \, dxdy$$

$$+ \frac{G_B t}{2} \int_0^L\int_0^b \left\{ 2(n-1)\left[\frac{\partial w}{\partial x}\frac{\partial \delta w}{\partial x} + \frac{\partial w}{\partial y}\frac{\partial \delta w}{\partial y}\right] - \frac{2}{t}\frac{\partial \delta w}{\partial x}\, \vec{B}^{\,*T} \cdot \vec{u}^{\,*} - \frac{2}{t}\frac{\partial \delta w}{\partial y}\, \vec{B}^{\,*T} \cdot \vec{v}^{\,*} \right\} dxdy$$

$$- \int_0^L\int_0^b [p\delta w]\, dxdy - \int_0^L\int_0^b \left[N_x \frac{\partial w}{\partial x}\frac{\partial \delta w}{\partial x}\right] dxdy = 0 \qquad (58)$$

Integration by parts leads to the following scalar differential equation

and associated boundary conditions.

$$-\frac{t}{R}\left[\vec{K}_{12}^{T}\cdot\frac{\partial\vec{u}^{*}}{\partial x}+\vec{K}_{23}^{T}\cdot\left(\frac{\partial\vec{v}^{*}}{\partial x}+\frac{\partial\vec{u}^{*}}{\partial y}\right)+\vec{K}_{22}^{T}\frac{\partial\vec{v}^{*}}{\partial y}\right]$$

$$+\frac{t}{R^{2}}\vec{I}^{T}\cdot\tilde{C}_{22}\cdot\vec{I}\,w-G_{B}t\,(n-1)\left[\frac{\partial^{2}w}{\partial x^{2}}+\frac{\partial^{2}w}{\partial y^{2}}\right]$$

$$+G_{B}\vec{B}^{*T}\cdot\left(\frac{\partial\vec{u}^{*}}{\partial x}+\frac{\partial\vec{v}^{*}}{\partial y}\right)+N_{x}\frac{\partial^{2}w}{\partial x^{2}}-p=0 \qquad (59)$$

At $x = 0,L$

$$\left\{G_{B}\left[t\,(n-1)\frac{\partial w}{\partial x}-\vec{B}^{*T}\cdot\vec{u}^{*}\right]-N_{x}\frac{\partial w}{\partial x}\right\}\delta w=0 \qquad (60)$$

At $y = 0,b$

$$G_{B}\left[t\,(n-1)\frac{\partial w}{\partial y}-\vec{B}^{*T}\cdot\vec{v}^{*}\right]\delta w=0 \qquad (61)$$

Variation of the total potential energy functional, Equation (29), with respect to the generalized displacement vector $\vec{u}^{*}$ gives

$$\begin{aligned}\delta_{\vec{u}^{*}}(U+V)=\int_{0}^{L}\int_{0}^{b}t\Bigg\{&\left(\tilde{C}_{11}^{*}\cdot\frac{\partial\vec{u}^{*}}{\partial x}\right)^{T}\cdot\frac{\partial\delta\vec{u}^{*}}{\partial x}+\left(\tilde{C}_{12}^{*}\cdot\frac{\partial\vec{v}^{*}}{\partial y}\right)^{T}\cdot\frac{\partial\delta\vec{u}^{*}}{\partial x}\\&+\left[\tilde{C}_{33}^{*}\cdot\left(\frac{\partial\vec{u}^{*}}{\partial y}+\frac{\partial\vec{v}^{*}}{\partial x}\right)\right]^{T}\cdot\frac{\partial\delta\vec{u}^{*}}{\partial y}+\left(\tilde{C}_{13}^{*}\cdot\frac{\partial\vec{v}^{*}}{\partial x}\right)^{T}\cdot\frac{\partial\delta\vec{u}^{*}}{\partial x}\\&+\left(\tilde{C}_{13}^{*}\cdot\frac{\partial\vec{u}^{*}}{\partial y}\right)^{T}\cdot\frac{\partial\delta\vec{u}^{*}}{\partial x}+\left(\tilde{C}_{13}^{*}\cdot\frac{\partial\vec{u}^{*}}{\partial x}\right)^{T}\cdot\frac{\partial\delta\vec{u}^{*}}{\partial y}\\&+\left(\tilde{C}_{23}^{*}\cdot\frac{\partial\vec{v}^{*}}{\partial y}\right)^{T}\cdot\frac{\partial\delta\vec{u}^{*}}{\partial y}-\frac{w}{R}\vec{K}_{12}^{T}\cdot\frac{\partial\delta\vec{u}^{*}}{\partial x}-\frac{w}{R}\vec{K}_{23}^{T}\cdot\frac{\partial\delta\vec{u}^{*}}{\partial y}\Bigg\}dxdy\\&+\int_{0}^{L}\int_{0}^{b}G_{B}\left\{-\frac{\partial w}{\partial x}\vec{B}^{*T}+\frac{1}{t}\left(\tilde{A}^{*}\cdot\vec{u}^{*}\right)^{T}\right\}\delta\vec{u}^{*}dxdy=0\end{aligned} \qquad (62)$$

where the identities expressed by Equation (30) have been utilized.

Integration by parts of Equation (62) leads to the following vector differential equation of equilibrium and associated vector boundary conditions.

$$
\begin{aligned}
&- t\,\tilde{C}^{*}_{11} \cdot \frac{\partial^2 \vec{u}^{\,*}}{\partial x^2} - t\,\tilde{C}^{*}_{12} \cdot \frac{\partial^2 \vec{v}^{\,*}}{\partial x \partial y} \\
&- t\,\tilde{C}^{*}_{33} \cdot \left(\frac{\partial^2 \vec{u}^{\,*}}{\partial y^2} + \frac{\partial^2 \vec{v}^{\,*}}{\partial x \partial y} \right) - t\,\tilde{C}^{*}_{13} \cdot \frac{\partial^2 \vec{v}^{\,*}}{\partial x^2} \\
&- 2t\,\tilde{C}^{*}_{13} \cdot \frac{\partial^2 \vec{u}^{\,*}}{\partial x \partial y} - t\,\tilde{C}^{*}_{23} \cdot \frac{\partial^2 \vec{v}^{\,*}}{\partial y^2} + \frac{t}{R}\,\vec{K}_{12}\,\frac{\partial w}{\partial x} \\
&+ \frac{t}{R}\,\vec{K}_{23}\,\frac{\partial w}{\partial y} - G_B\,\vec{B}^{\,*}\,\frac{\partial w}{\partial x} + \frac{G_B}{t}\,\tilde{A}^{*} \cdot \vec{u}^{\,*} = 0
\end{aligned}
\tag{63}
$$

At $x = 0, L$

$$
\left\{ t\,\tilde{C}^{*}_{11} \cdot \frac{\partial \vec{u}^{\,*}}{\partial x} + t\,\tilde{C}^{*}_{12} \cdot \frac{\partial \vec{v}^{\,*}}{\partial y} + t\,\tilde{C}^{*}_{13} \cdot \left(\frac{\partial \vec{v}^{\,*}}{\partial x} + \frac{\partial \vec{u}^{\,*}}{\partial y} \right) - \vec{K}_{12}\,\frac{w}{R} \right\} \cdot \delta \vec{u}^{\,*T} = 0 \tag{64}
$$

At $y = 0, b$

$$
\left\{ t\,\tilde{C}^{*}_{33} \cdot \left(\frac{\partial \vec{u}^{\,*}}{\partial y} + \frac{\partial \vec{v}^{\,*}}{\partial x} \right) + t\,\tilde{C}^{*}_{13} \cdot \frac{\partial \vec{u}^{\,*}}{\partial x} + t\,\tilde{C}^{*}_{23} \cdot \frac{\partial \vec{v}^{\,*}}{\partial y} - \vec{K}_{23}\,\frac{w}{R} \right\} \cdot \delta \vec{u}^{\,*T} = 0 \tag{65}
$$

Variation of the total potential energy functional, Equation (29), with

respect to the generalized displacement vector $\vec{v}^*$ gives

$$\delta_{\vec{v}^*}(U + V) = \int_0^L \int_0^b t \left\{ \left(\tilde{C}^*_{22} \cdot \frac{\partial \vec{v}^*}{\partial y} \right)^T \cdot \frac{\partial \delta \vec{v}^*}{\partial y} + \left(\tilde{C}^*_{12} \cdot \frac{\partial \vec{u}^*}{\partial x} \right)^T \cdot \frac{\partial \delta \vec{v}^*}{\partial y} \right.$$

$$+ \left[\tilde{C}^*_{33} \cdot \left(\frac{\partial \vec{u}^*}{\partial y} + \frac{\partial \vec{v}^*}{\partial x} \right) \right]^T \cdot \frac{\partial \delta \vec{v}^*}{\partial x} + \left(\tilde{C}^*_{23} \cdot \frac{\partial \vec{u}^*}{\partial y} \right)^T \cdot \frac{\partial \delta \vec{v}^*}{\partial y}$$

$$+ \left(\tilde{C}^*_{23} \cdot \frac{\partial \vec{v}^*}{\partial x} \right)^T \cdot \frac{\partial \delta \vec{v}^*}{\partial y} + \left(\tilde{C}^*_{23} \cdot \frac{\partial \vec{v}^*}{\partial y} \right)^T \cdot \frac{\partial \delta \vec{v}^*}{\partial x}$$

$$+ \left(\tilde{C}^*_{13} \cdot \frac{\partial \vec{u}^*}{\partial x} \right)^T \cdot \frac{\partial \delta \vec{v}^*}{\partial x} - \frac{w}{R} \vec{K}^T_{23} \cdot \frac{\partial \delta \vec{v}^*}{\partial x}$$

$$\left. - \frac{w}{R} \vec{K}^T_{22} \cdot \frac{\partial \delta \vec{v}^*}{\partial y} \right\} dxdy + \int_0^L \int_0^b G_B \left\{ - \frac{\partial w}{\partial y} \vec{B}^{*T} \right.$$

$$\left. + \frac{1}{t} \left(\tilde{A}^* \cdot \vec{v}^* \right)^T \right\} \delta \vec{v}^* \, dxdy = 0 \qquad (66)$$

where the identities expressed by Equation (30) have been utilized.

Integration by parts leads to the following vector differential equation and associated vector boundary conditions.

$$- t \tilde{C}^*_{22} \cdot \frac{\partial^2 \vec{v}^*}{\partial y^2} - t \tilde{C}^*_{12} \cdot \frac{\partial^2 \vec{u}^*}{\partial x \partial y}$$

$$- t \tilde{C}^*_{33} \cdot \left(\frac{\partial^2 \vec{v}^*}{\partial x^2} + \frac{\partial^2 \vec{u}^*}{\partial x \partial y} \right) - t \tilde{C}^*_{23} \cdot \frac{\partial^2 \vec{u}^*}{\partial y^2}$$

$$- 2t \tilde{C}^*_{23} \cdot \frac{\partial^2 \vec{v}^*}{\partial x \partial y} - t \tilde{C}^*_{13} \cdot \frac{\partial^2 \vec{u}^*}{\partial x^2} + \frac{t}{R} \vec{K}_{23} \frac{\partial w}{\partial x}$$

$$+ \frac{t}{R} \vec{K}_{22} \frac{\partial w}{\partial y} - G_B \vec{B}^* \frac{\partial w}{\partial y} + \frac{G_B}{t} \tilde{A}^* \cdot \vec{v}^* = 0 \qquad (67)$$

At $x = 0, L$

$$\left\{ t\, \tilde{C}^{*}_{33} \cdot \left(\frac{\partial \vec{u}^{\,*}}{\partial y} + \frac{\partial \vec{v}^{\,*}}{\partial x} \right) + t\, \tilde{C}^{*}_{23} \cdot \frac{\partial \vec{v}^{\,*}}{\partial y} + t\, \tilde{C}^{*}_{13} \frac{\partial \vec{u}^{\,*}}{\partial x} - \vec{K}_{23} \frac{w}{R} \right\} \cdot \delta \vec{v}^{\,*T} = 0 \qquad (68)$$

At $y = 0, b$

$$\left\{ t\, \tilde{C}^{*}_{22} \cdot \frac{\partial \vec{v}^{\,*}}{\partial y} + t\, \tilde{C}^{*}_{12} \cdot \frac{\partial \vec{u}^{\,*}}{\partial x} + t\, \tilde{C}^{*}_{23} \cdot \frac{\partial \vec{u}^{\,*}}{\partial y} + t\, \tilde{C}^{*}_{23} \frac{\partial \vec{v}^{\,*}}{\partial x} - \vec{K}_{22} \frac{w}{R} \right\} \cdot \delta \vec{v}^{\,*T} = 0 \qquad (69)$$

Again it is noted that in Equation (59), $N_x = 0$ when bending problems are considered and $p = 0$ when axial compression buckling problems are considered.

APPENDIX IV

METHOD OF SOLUTION FOR FLAT PLATES WITH ANISOTROPIC LAMINAE

For rectangular plates in which some fibers are not oriented parallel to the plate edges, the governing differential equations do not possess a closed-form solution consistent with the boundary conditions of simple support. Consequently, for this type of construction, a Rayleigh-Ritz procedure is used in conjunction with the functional given by Equation (29) to effect an approximate solution.

The vectors $\vec{u}^*$ and $\vec{v}^*$ and the scalar function w are approximated by

$$\left.\begin{aligned} \vec{u}^* &= \vec{e}_1\alpha_1 + \vec{e}_2\alpha_2 + \ldots + \vec{e}_k\alpha_k \\ \vec{v}^* &= \vec{f}_1\beta_1 + \vec{f}_2\beta_2 + \ldots + \vec{f}_k\beta_k \\ w &= g_1\gamma_1 + g_2\gamma_2 + \ldots + g_k\gamma_k \end{aligned}\right\} \tag{70}$$

where

$$\left.\begin{aligned} \alpha_j &= \alpha_j(x,y) \\ \beta_j &= \beta_j(x,y) \\ \gamma_j &= \gamma_j(x,y) \end{aligned}\right\} \tag{71}$$

with

$$\tilde{\alpha} = \begin{bmatrix} \alpha_1 & \alpha_2 & \ldots & \alpha_k & 0 & 0 & \ldots & 0 & & \ldots & & \\ 0 & 0 & \ldots & 0 & \alpha_1 & \alpha_2 & \ldots & \alpha_k & 0 & 0 \ldots & 0 & \ldots \\ & & \vdots & & & & & & & & & \\ 0 & 0 & \ldots & 0 & & & \ldots & & 0 & 0 \ldots & 0 & \alpha_1 \; \alpha_2 \ldots \alpha_k \end{bmatrix} \tag{72}$$

$$\tilde{\beta} = \begin{bmatrix} \beta_1 & \beta_2 & \cdots & \beta_k & 0 & 0 & \cdots & 0 & & \cdots & & & \\ 0 & 0 & \cdots & 0 & \beta_1 & \beta_2 & \cdots & \beta_k & 0 & 0 \cdots 0 & & & \cdots \\ & & \vdots & & & & & & & & & & \\ 0 & 0 & \cdots & 0 & & & \cdots & & 0 & 0 \cdots 0 & \beta_1 & \beta_2 \cdots & \beta_k \end{bmatrix} \tag{73}$$

$$\vec{\gamma} = \begin{bmatrix} \gamma_1 \\ \gamma_2 \\ \vdots \\ \gamma_k \end{bmatrix} \tag{74}$$

$$\vec{e} = \begin{bmatrix} e_{11} \\ e_{12} \\ \vdots \\ e_{1k} \\ e_{21} \\ \vdots \\ e_{2k} \\ \vdots \\ e_{kk} \end{bmatrix} \tag{75}$$

$$\vec{f} = \begin{bmatrix} f_{11} \\ f_{12} \\ \vdots \\ f_{1k} \\ f_{21} \\ \vdots \\ f_{2k} \\ \vdots \\ f_{kk} \end{bmatrix} \tag{76}$$

and

$$\vec{g} = \begin{bmatrix} g_1 \\ g_2 \\ \vdots \\ g_k \end{bmatrix} \tag{77}$$

Equations (70) can be written as

$$\left.\begin{aligned} \vec{u}^{\,*} &= \tilde{\alpha} \cdot \vec{e} \\ \vec{v}^{\,*} &= \tilde{\beta} \cdot \vec{f} \\ w &= \vec{\gamma}^{\,T} \cdot \vec{g} \end{aligned}\right\} \tag{78}$$

With the introduction of Equations (78) into Equations (29) with $R \to \infty$ and cognizance taken of the identities, Equations (30), the total potential energy becomes

$$U + V = \frac{t}{2} \int_0^L \int_0^b \left\{ \vec{e}^{\,T} \cdot \left(\tilde{\Phi}_1 + \tilde{\Phi}_6 + 2\tilde{\Phi}_4 + \frac{G_B}{t^2}\, \tilde{\Phi}_{12} \right) \cdot \vec{e} \right.$$

(Cont'd)

$$+ \vec{f}^T \cdot \left(\tilde{\Phi}_2 + \tilde{\Phi}_9 + 2\tilde{\Phi}_{11} + \frac{G_B}{t^2} \tilde{\Phi}_{13} \right) \cdot \vec{f}$$

$$+ \vec{e}^T \cdot \left(\tilde{\Phi}_7 + 2\tilde{\Phi}_3 + 2\tilde{\Phi}_5 \right) \cdot \vec{f} + \vec{f}^T \cdot \left(\tilde{\Phi}_8 + 2\tilde{\Phi}_{10} \right) \cdot \vec{e}$$

$$+ (n-1)\, G_B\, \vec{g}^T \cdot \left(\vec{\gamma}_{,x} \cdot \vec{\gamma}_{,x}^T + \vec{\gamma}_{,y} \cdot \vec{\gamma}_{,y}^T \right) \cdot \vec{g}$$

$$- \frac{2G_B}{t} \left(\vec{g}^T \cdot \tilde{\Phi}_{14} \cdot \vec{e} + \vec{g}^T \cdot \tilde{\Phi}_{15} \cdot \vec{f} \right) \Bigg\} dxdy$$

$$- \int_0^L \int_0^b \left\{ \frac{N_x}{2} \left(\vec{g}^T \cdot \vec{\gamma}_{,x} \cdot \vec{\gamma}_{,x}^T \cdot \vec{g} \right) + p\vec{g}^T \cdot \vec{\gamma} \right\} dxdy \qquad (79)$$

where

$$\left.\begin{aligned}
\tilde{\Phi}_1 &= \tilde{\alpha}_{,x}^T \cdot \tilde{C}_{11}^* \cdot \tilde{\alpha}_{,x} \\
\tilde{\Phi}_2 &= \tilde{\beta}_{,y}^T \cdot \tilde{C}_{22}^* \cdot \tilde{\beta}_{,y} \\
\tilde{\Phi}_3 &= \tilde{\alpha}_{,x}^T \cdot \tilde{C}_{12}^* \cdot \tilde{\beta}_{,y} \\
\tilde{\Phi}_4 &= \tilde{\alpha}_{,x}^T \cdot \tilde{C}_{13}^* \cdot \tilde{\alpha}_{,y} \\
\tilde{\Phi}_5 &= \tilde{\alpha}_{,x}^T \cdot \tilde{C}_{13}^* \cdot \tilde{\beta}_{,x} \\
\tilde{\Phi}_6 &= \tilde{\alpha}_{,y}^T \cdot \tilde{C}_{33}^* \cdot \tilde{\alpha}_{,y} \\
\tilde{\Phi}_7 &= \tilde{\alpha}_{,y}^T \cdot \tilde{C}_{33}^* \cdot \tilde{\beta}_{,x} \\
\tilde{\Phi}_8 &= \tilde{\beta}_{,x}^T \cdot \tilde{C}_{33}^* \cdot \tilde{\alpha}_{,y} \\
\tilde{\Phi}_9 &= \tilde{\beta}_{,x}^T \cdot \tilde{C}_{33}^* \cdot \tilde{\beta}_{,x} \\
\tilde{\Phi}_{10} &= \tilde{\beta}_{,y}^T \cdot \tilde{C}_{23}^* \cdot \tilde{\alpha}_{,y}
\end{aligned}\right\} \qquad (80)$$

(Cont'd)

$$\left.\begin{aligned}
\tilde{\Phi}_{11} &= \tilde{\beta}^{T}_{,y} \cdot \tilde{C}^{*}_{23} \cdot \tilde{\beta}_{,x} \\
\tilde{\Phi}_{12} &= \tilde{\alpha}^{T} \cdot \tilde{A}^{*} \cdot \tilde{\alpha} \\
\tilde{\Phi}_{13} &= \tilde{\beta}^{T} \cdot \tilde{A}^{*} \cdot \tilde{\beta} \\
\tilde{\Phi}_{14} &= \vec{\gamma}_{,x} \cdot \vec{B}^{*T} \cdot \tilde{\alpha} \\
\tilde{\Phi}_{15} &= \vec{\gamma}_{,y} \cdot \vec{B}^{*T} \cdot \tilde{\beta}
\end{aligned}\right\}$$

Due to the form of $\tilde{\alpha}$ and $\tilde{\beta}$ as given by Equations (72) and (73), the matrices $\tilde{\Phi}_j$ given in Equations (80) have, in turn, a special form. These matrices are equivalent to partitioned matrices in which the number of submatrices equals the number of elements in $\tilde{C}^{*}_{ij}$, or $\tilde{A}^{*}$ and $\vec{B}^{*T}$, respectively.

With

$$\vec{\alpha} = \begin{bmatrix} \alpha_1 \\ \alpha_2 \\ \vdots \\ \alpha_k \end{bmatrix} \tag{81}$$

$$\vec{\beta} = \begin{bmatrix} \beta_1 \\ \beta_2 \\ \vdots \\ \beta_k \end{bmatrix} \tag{82}$$

and $\vec{\gamma}$ as given by Equation (74), the submatrices are formed by multiplying their corresponding elements in $\tilde{C}^{*}_{ij}$ by the matrix product involving the vectors $\vec{\alpha}$, $\vec{\beta}$, and $\vec{\gamma}$ or their derivatives. For example,

with $\tilde{C}^*_{11}$ assumed to be a 2 x 2 matrix, $\tilde{\Phi}_1$ is formed from four sub-matrices given by the respective element of $\tilde{C}^*_{11}$ times the matrix $\vec{\alpha}_{,x} \cdot \vec{\alpha}^T_{,x}$.

Upon performing the integrations

$$\left.\begin{aligned}
\tilde{S}_1 &= \int_0^L\int_0^b \left(\tilde{\Phi}_1 + \tilde{\Phi}_6 + 2\Phi_4 + \frac{G_B}{t^2}\,\tilde{\Phi}_{12}\right) dxdy \\
\tilde{S}_2 &= \int_0^L\int_0^b \left(\tilde{\Phi}_2 + \tilde{\Phi}_9 + 2\tilde{\Phi}_{11} + \frac{G_B}{t^2}\,\tilde{\Phi}_{13}\right) dxdy \\
\tilde{S}_3 &= \int_0^L\int_0^b \left(\tilde{\Phi}_7 + 2\tilde{\Phi}_3 + 2\tilde{\Phi}_5\right) dxdy \\
\tilde{S}_4 &= \int_0^L\int_0^b \left(\tilde{\Phi}_8 + 2\tilde{\Phi}_{10}\right) dxdy \\
\tilde{S}_5 &= \frac{2G_B}{t} \int_0^L\int_0^b \tilde{\Phi}_{14}\, dxdy \\
\tilde{S}_6 &= \frac{2G_B}{t} \int_0^L\int_0^b \Phi_{15}\, dxdy \\
\tilde{S}_7 &= (n-1)\, G_B \int_0^L\int_0^b \left(\vec{\gamma}_{,x} \cdot \vec{\gamma}^T_{,x} + \vec{\gamma}_{,y} \cdot \vec{\gamma}^T_{,y}\right) dxdy
\end{aligned}\right\} \quad (83)$$

the total potential energy given by Equation (79) becomes

$$\begin{aligned}
U + V = \frac{t}{2} \Big\{ & \vec{e}^T \cdot \tilde{S}_1 \cdot \vec{e} + \vec{f}^T \cdot \tilde{S}_2 \cdot \vec{f} + \vec{e}^T \cdot \tilde{S}_3 \cdot \vec{f} \\
& + \vec{f}^T \cdot \tilde{S}_4 \cdot \vec{e} - \vec{g}^T \cdot \tilde{S}_5 \cdot \vec{e} - \vec{g}^T \cdot \tilde{S}_6 \cdot \vec{f} + \vec{g}^T \cdot \tilde{S}_7 \cdot \vec{g} \Big\} \\
& - \int_0^L\int_0^b \left[\frac{N_x}{2}\left(\vec{g}^T \cdot \vec{\gamma}_{,x} \cdot \vec{\gamma}^T_{,x} \cdot \vec{g}\right) + p\vec{g}^T \cdot \vec{\gamma}\right] dxdy \qquad (84)
\end{aligned}$$

Extremization of $(U + V)$ with respect to $\vec{e}$, $\vec{f}$ and $\vec{g}$ leads to the following vector equations:

$$\frac{t}{2}\left[\left(\tilde{S}_1 + \tilde{S}_1^T\right)\cdot\vec{e} + \left(\tilde{S}_3 + \tilde{S}_4^T\right)\cdot\vec{f} - \tilde{S}_5^T\cdot\vec{g}\right] = 0 \qquad (85)$$

$$\frac{t}{2}\left[\left(\tilde{S}_3^T + \tilde{S}_4\right)\cdot\vec{e} + \left(\tilde{S}_2^T + \tilde{S}_2\right)\cdot\vec{f} - \tilde{S}_6^T\cdot\vec{g}\right] = 0 \qquad (86)$$

$$\frac{t}{2}\left[-\tilde{S}_5\cdot\vec{e} - \tilde{S}_6\cdot\vec{f} + \left(\tilde{S}_7 + \tilde{S}_7^T\right)\cdot\vec{g}\right] - \int_0^L\int_0^b \left[N_x\vec{\gamma}_{,x}\cdot\vec{\gamma}_{,x}^T\cdot\vec{g} + p\,\vec{\gamma}\right] dxdy = 0 \qquad (87)$$

The characteristic functions γ_j, α_j, and β_j $(j = 1,2,3,4)$ given by Equations (74), (81) and (82), respectively, are now taken as

$$\left.\begin{aligned} \alpha_j &= \cos\frac{j\pi x}{L}\sin\frac{j\pi y}{b} \\ \beta_j &= \sin\frac{j\pi x}{L}\cos\frac{j\pi y}{b} \\ \gamma_j &= \sin\frac{j\pi x}{L}\sin\frac{j\pi y}{b} \\ j &= 1,2,3,4 \end{aligned}\right\} \qquad (88)$$

In view of Equations (80) and (88), the integration of the matrix integrals $\tilde{S}_j$ $(j = 1,2,\ldots,7)$, Equations (83), can be effected with respect to the functions α_j, β_j, and γ_j. Subsequent substitution of the integrated $\tilde{S}_j$ functions $(j = 1,2,\ldots,7)$ into the Euler equations, Equations (85) through (87), leads to a set of algebraic equations. The solution of these algebraic equations yields the desired vectors $\vec{e}$, $\vec{f}$, and $\vec{g}$.

APPENDIX V

EXPANSION OF GOVERNING EQUATIONS AND BOUNDARY CONDITIONS CORRESPONDING TO A FIRST APPROXIMATION (m = 1) FOR FLAT PLATES ($R \to \infty$); REDUCTION TO REISSNER PLATE THEORY

With the definitions

$$\left.\begin{aligned} A_{ij} &= \sum_{k=1}^{n} t\, C_{ij}^{(k)} \\ B_{ij} &= \sum_{k=1}^{n} z_k t\, C_{ij}^{(k)} \\ D_{ij} &= \sum_{k=1}^{n} z_k^2 t\, C_{ij}^{(k)} \\ & \qquad\qquad \begin{matrix} i = 1,2,3 \\ j = 1,2,3 \end{matrix} \end{aligned}\right\} \tag{89}$$

and $m = 1$, the governing differential equations, Equations (31) through (33), can be expanded to give the following five governing scalar equations for the bending ($N_x = 0$) of flat plates ($R \to \infty$).

$$\begin{aligned} -\Bigg[& A_{11}\frac{\partial^2 u_0^*}{\partial x^2} + 2A_{13}\frac{\partial^2 u_0^*}{\partial x \partial y} + A_{33}\frac{\partial^2 u_0^*}{\partial y^2} \\ & + A_{13}\frac{\partial^2 v_0^*}{\partial x^2} + (A_{12} + A_{33})\frac{\partial^2 v_0^*}{\partial x \partial y} + A_{23}\frac{\partial^2 v_0^*}{\partial y^2} \\ & + B_{11}\frac{\partial^2 u_1^*}{\partial x^2} + 2B_{13}\frac{\partial^2 u_1^*}{\partial x \partial y} + B_{33}\frac{\partial^2 u_1^*}{\partial y^2} \\ & + B_{13}\frac{\partial^2 v_1^*}{\partial x^2} + (B_{12} + B_{33})\frac{\partial^2 v_1^*}{\partial x \partial y} + B_{23}\frac{\partial^2 v_1^*}{\partial y^2} \Bigg] = 0 \end{aligned} \tag{90}$$

$$- \left[A_{13} \frac{\partial^2 u_0^*}{\partial x^2} + (A_{12} + A_{33}) \frac{\partial^2 u_0^*}{\partial x \partial y} + A_{23} \frac{\partial^2 u_0^*}{\partial y^2} \right.$$

$$+ A_{33} \frac{\partial^2 v_0^*}{\partial x^2} + 2A_{33} \frac{\partial^2 v_0^*}{\partial x \partial y} + A_{22} \frac{\partial^2 v_0^*}{\partial y^2}$$

$$+ B_{13} \frac{\partial^2 u_1^*}{\partial x^2} + (B_{12} + B_{33}) \frac{\partial^2 u_1^*}{\partial x \partial y} + B_{23} \frac{\partial^2 u_1^*}{\partial y^2}$$

$$\left. + B_{33} \frac{\partial^2 v_1^*}{\partial x^2} + 2B_{23} \frac{\partial^2 v_1^*}{\partial x \partial y} + B_{22} \frac{\partial^2 v_1^*}{\partial y^2} \right] = 0 \qquad (91)$$

$$- \left[B_{11} \frac{\partial^2 u_0^*}{\partial x^2} + 2B_{13} \frac{\partial^2 u_0^*}{\partial x \partial y} + B_{33} \frac{\partial^2 u_0^*}{\partial y^2} \right.$$

$$+ B_{13} \frac{\partial^2 v_0^*}{\partial x^2} + (B_{12} + B_{33}) \frac{\partial^2 v_0^*}{\partial x \partial y} + B_{23} \frac{\partial^2 v_0^*}{\partial y^2}$$

$$+ D_{11} \frac{\partial^2 u_1^*}{\partial x^2} + 2D_{13} \frac{\partial^2 u_1^*}{\partial x \partial y} + D_{33} \frac{\partial^2 u_1^*}{\partial y^2}$$

$$\left. + D_{13} \frac{\partial^2 v_1^*}{\partial x^2} + (D_{12} + D_{33}) \frac{\partial^2 v_1^*}{\partial x \partial y} + D_{23} \frac{\partial^2 v_1^*}{\partial y^2} \right]$$

$$+ (n-1) G_B t \left(u_1 - \frac{\partial w}{\partial x} \right) = 0 \qquad (92)$$

$$- \left[B_{13} \frac{\partial^2 u_0^*}{\partial x^2} + (B_{33} + B_{12}) \frac{\partial^2 u_0^*}{\partial x \partial y} + B_{23} \frac{\partial^2 u_0^*}{\partial y^2} \right.$$

$$+ B_{33} \frac{\partial^2 v_0^*}{\partial x^2} + 2B_{23} \frac{\partial^2 v_0^*}{\partial x \partial y} + B_{22} \frac{\partial^2 v_0^*}{\partial y^2}$$

$$+ D_{13} \frac{\partial^2 u_1^*}{\partial x^2} + (D_{33} + D_{12}) \frac{\partial^2 u_1^*}{\partial x \partial y} + D_{23} \frac{\partial^2 u_1^*}{\partial y^2}$$

$$\left. + D_{33} \frac{\partial^2 v_1^*}{\partial x^2} + 2D_{33} \frac{\partial^2 v_1^*}{\partial x \partial y} + D_{22} \frac{\partial^2 v_1^*}{\partial y^2} \right]$$

$$+ (n-1) G_B t \left(v_1^* - \frac{\partial w}{\partial y} \right) = 0 \qquad (93)$$

$$- (n-1) G_B t \left[\frac{\partial^2 w}{\partial x^2} + \frac{\partial^2 w}{\partial y^2} - \frac{\partial u_1^*}{\partial x} - \frac{\partial v_1^*}{\partial y} \right] - p = 0 \qquad (94)$$

The boundary conditions associated with Equations (90) through (94) are obtained by expanding Equations (34) through (39) for $m = 1$ and $R \to \infty$. These expansions are straightforward and result in the following scalar equations.

At $x = 0, L$

$$\left[A_{11} \frac{\partial u_0^*}{\partial x} + A_{12} \frac{\partial v_0^*}{\partial y} + A_{13} \left(\frac{\partial u_0^*}{\partial y} + \frac{\partial v_0^*}{\partial x} \right) \right.$$

$$\left. + B_{11} \frac{\partial u_1^*}{\partial x} + B_{12} \frac{\partial v_1^*}{\partial y} + B_{13} \left(\frac{\partial u_1^*}{\partial y} + \frac{\partial v_1^*}{\partial x} \right) \right] \cdot \delta u_0^* = 0$$

$$\left[A_{33} \left(\frac{\partial v_0^*}{\partial x} + \frac{\partial u_0^*}{\partial y} \right) + A_{23} \frac{\partial v_0^*}{\partial y} + A_{13} \frac{\partial u_0^*}{\partial x} \right. \qquad \text{(Cont'd)}$$

$$+ B_{33}\left(\frac{\partial u_1^*}{\partial y} + \frac{\partial v_1^*}{\partial x}\right) + B_{23}\frac{\partial v_1^*}{\partial y} + B_{13}\frac{\partial u_1^*}{\partial x}\Bigg] \cdot \delta v_0^* = 0$$

$$\Bigg[B_{11}\frac{\partial u_0^*}{\partial x} + B_{12}\frac{\partial v_0^*}{\partial y} + B_{13}\left(\frac{\partial u_0^*}{\partial y} + \frac{\partial v_0^*}{\partial x}\right)$$

$$+ D_{11}\frac{\partial u_1^*}{\partial x} + D_{12}\frac{\partial v_1^*}{\partial y} + D_{13}\left(\frac{\partial u_1^*}{\partial y} + \frac{\partial v_1^*}{\partial x}\right)\Bigg] \cdot \delta u_1^* = 0$$

$$\Bigg[B_{33}\left(\frac{\partial u_0^*}{\partial y} + \frac{\partial v_0^*}{\partial x}\right) + B_{23}\frac{\partial v_0^*}{\partial y} + B_{13}\frac{\partial u_0^*}{\partial x}$$

$$+ D_{33}\left(\frac{\partial u_1^*}{\partial y} + \frac{\partial v_1^*}{\partial x}\right) + D_{13}\frac{\partial u_1^*}{\partial x} + D_{23}\frac{\partial v_1^*}{\partial y}\Bigg] \cdot \delta v_1^* = 0$$

$$(n-1)\, G_B t\left(\frac{\partial w}{\partial x} - u_1^*\right) \cdot \delta w = 0 \qquad (95)$$

At $y = 0, b$

$$\Bigg[A_{33}\left(\frac{\partial u_0^*}{\partial y} + \frac{\partial v_0^*}{\partial x}\right) + A_{13}\frac{\partial u_0^*}{\partial x} + A_{23}\frac{\partial v_0^*}{\partial y}$$

$$+ B_{33}\left(\frac{\partial u_1^*}{\partial y} + \frac{\partial v_1^*}{\partial x}\right) + B_{13}\frac{\partial u_1^*}{\partial x} + B_{23}\frac{\partial v_1^*}{\partial y}\Bigg] \cdot \delta u_0^* = 0$$

$$\Bigg[A_{22}\frac{\partial v_0^*}{\partial y} + A_{12}\frac{\partial u_0^*}{\partial x} + A_{23}\left(\frac{\partial v_0^*}{\partial x} + \frac{\partial u_0^*}{\partial y}\right)$$

$$+ D_{22}\frac{\partial v_1^*}{\partial y} + D_{12}\frac{\partial u_1^*}{\partial x} + D_{23}\left(\frac{\partial v_1^*}{\partial x} + \frac{\partial u_1^*}{\partial y}\right)\Bigg] \cdot \delta v_0^* = 0$$

$$\Bigg[B_{33}\left(\frac{\partial u_0^*}{\partial y} + \frac{\partial v_0^*}{\partial x}\right) + B_{13}\frac{\partial u_0^*}{\partial x} + B_{23}\frac{\partial v_0^*}{\partial y} \qquad \text{(Cont'd)} \qquad (96)$$

$$
\left.
\begin{aligned}
&+ D_{33}\left(\frac{\partial v_1^*}{\partial y} + \frac{\partial u_1^*}{\partial x}\right) + D_{13}\frac{\partial u_1^*}{\partial x} + D_{23}\frac{\partial v_1^*}{\partial y}\Bigg] \cdot \delta u_1^* = 0 \\
&\Bigg[B_{22}\frac{\partial v_0^*}{\partial y} + B_{12}\frac{\partial u_0^*}{\partial x} + B_{23}\left(\frac{\partial u_0^*}{\partial y} + \frac{\partial v_0^*}{\partial x}\right) \\
&+ D_{22}\frac{\partial v_1^*}{\partial y} + D_{12}\frac{\partial u_1^*}{\partial x} + D_{23}\left(\frac{\partial u_1^*}{\partial y} + \frac{\partial v_1^*}{\partial x}\right)\Bigg] \cdot \delta v_1^* = 0 \\
&(n-1)\, G_B t\left(\frac{\partial w}{\partial y} - v_1^*\right) \cdot \delta w = 0
\end{aligned}
\right\}
$$

For plates symmetric about their reference planes, the material constants B_{ij} vanish. Consequently, the membrane displacements, u_0^* and v_0^*, and the bending displacements, u_1^*, v_1^*, and w, uncouple and only Equations (92), (93) and (94) are required to describe the plate behavior. In addition, for homogeneous plates $(n \to \infty,\ t \to 0)$, the material constants become

$$
\left.
\begin{aligned}
D_{13} &= D_{23} = 0 \\
D_{11} &= D_{22} = D \\
D_{12} &\to \nu D \\
D_{33} &\to \frac{D}{2(1+\nu)} \\
(n-1)\, tG_B &\to \frac{Eh}{2(1+\nu)}
\end{aligned}
\right\} \qquad (97)
$$

Thus, for homogeneous plates, Equations (92) through (94) reduce to

$$-D\left[\frac{\partial^2 u_1^*}{\partial x^2}+\frac{1-\nu}{2}\frac{\partial^2 u_1^*}{\partial y^2}+\frac{1+\nu}{2}\frac{\partial^2 v_1^*}{\partial x\partial y}\right]+\frac{Eh}{2(1+\nu)}\left(u_1^*-\frac{\partial w}{\partial x}\right)=0 \quad (98)$$

$$-D\left[\frac{\partial^2 v_1^*}{\partial y^2}+\frac{1-\nu}{2}\frac{\partial^2 v_1^*}{\partial x^2}+\frac{1+\nu}{2}\frac{\partial^2 u_1^*}{\partial x\partial y}\right]+\frac{Eh}{2(1+\nu)}\left(v_1^*-\frac{\partial w}{\partial y}\right)=0 \quad (99)$$

$$-\frac{Eh}{2(1+\nu)}\left[\frac{\partial^2 w}{\partial x^2}+\frac{\partial^2 w}{\partial y^2}-\left(\frac{\partial u_1^*}{\partial x}+\frac{\partial v_1^*}{\partial y}\right)\right]-p=0 \quad (100)$$

Differentiation of Equations (98) and (99) with respect to x and y, respectively, and summation of the two resulting equations lead to

$$-D\left[\left(\frac{\partial^2}{\partial x^2}+\frac{\partial^2}{\partial y^2}\right)\left(\frac{\partial u_1^*}{\partial x}+\frac{\partial v_1^*}{\partial y}\right)\right]=\frac{Eh}{2(1+\nu)}\left[\left(\frac{\partial^2 w}{\partial x^2}+\frac{\partial^2 w}{\partial y^2}\right)-\left(\frac{\partial u_1^*}{\partial x}+\frac{\partial v_1^*}{\partial y}\right)\right] \quad (101)$$

Equation (100) gives

$$\left(\frac{\partial u_1^*}{\partial x}+\frac{\partial v_1^*}{\partial y}\right)=\frac{2(1+\nu)p}{EA}+\frac{\partial^2 w}{\partial x^2}+\frac{\partial^2 w}{\partial y^2} \quad (102)$$

Then, substitution of Equations (102) into Equation (101) results in

$$D\nabla^4 w=-\frac{h^2}{6(1-\nu)}\nabla^2 p+p \quad (103)$$

Equation (103) is of the same form as the governing equation in Reissner plate theory.[17] The only difference between Equation (103) and the governing equation of the Reissner plate theory appears in the coefficient of the first term on the right-hand side of the equation. This coefficient is slightly different in the Reissner theory because the transverse shearing stresses are assumed therein to vary parabolically through the cross section. For $m = 1$ in the present analysis, the transverse shearing stresses are constant through the thickness of the plate.